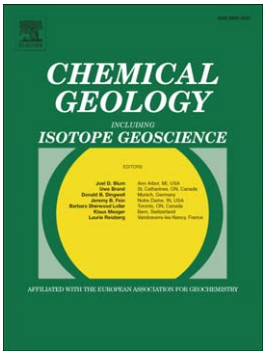

Subduction Zone Metamorphic Pathway for Deep Carbon Cycling: II. Evidence from HP/UHP Metabasaltic Rocks and Ophicarbonates

Nathan C. Collins, Gray E. Bebout, Samuel Angiboust, Philippe Agard, Marco Scambelluri, Laura Crispini, Timm John

PII: S0009-2541(15)00299-5
DOI: doi: 10.1016/j.chemgeo.2015.06.012
Reference: CHEMGE 17607

To appear in: *Chemical Geology*

Received date: 10 February 2015
Revised date: 8 June 2015
Accepted date: 9 June 2015

Please cite this article as: Collins, Nathan C., Bebout, Gray E., Angiboust, Samuel, Agard, Philippe, Scambelluri, Marco, Crispini, Laura, John, Timm, Subduction Zone Metamorphic Pathway for Deep Carbon Cycling: II. Evidence from HP/UHP Metabasaltic Rocks and Ophicarbonates, *Chemical Geology* (2015), doi: 10.1016/j.chemgeo.2015.06.012

Subduction Zone Metamorphic Pathway for Deep Carbon Cycling: II. Evidence from HP/UHP Metabasaltic Rocks and Ophicarbonates

Nathan C. Collins[1], Gray E. Bebout[1], Samuel Angiboust[2], Philippe Agard[3], Marco Scambelluri[4], Laura Crispini[4], Timm John[5]

[1]Department of Earth and Environmental Sciences, Lehigh University, Bethlehem, Pennsylvania, 18015, U.S.A. (corresponding author; telephone: 610-758-5831; FAX: 610-758-3677; e-mail: geb0@lehigh.edu)

[2]GeoForschungsZentrum (GFZ), Telegrafenberg, D-14473 Potsdam, Germany

[3]ISTEP, Université Paris 06-UPMC, UMR CNRS 7193, 4 place Jussieu, F-75005, Paris, France

[4]Dip.Te.Ris Università degli Studi di Genova Via Balbi, 5 - 16126 Genova, Italy

[5]Institut für Geologische Wissenschaften, Malteserstrasse 74-100, D-12249 Berlin, Germany

revision for *Chemical Geology* (6-05-15)

Abstract

Exposures of low-grade metabasalts and ophicarbonates in the Northern Apennines, and their high- and ultrahigh-pressure metamorphic equivalents in the Western and Ligurian Alps and Tianshan (representing an overall peak *P-T* range of ~0.2-3.0 GPa, 200-610°C), allow investigation of the effects of prograde metamorphic devolatilization, and other fluid-rock interactions, on degrees of retention and isotopic evolution of C in subducting oceanic crust and associated mantle rocks. Such work can inform models of C cycling at convergent margins, helping constrain the efficiency of return of initially subducted C via arc volcanism and the fraction of this subducted C entering the deeper mantle beyond arcs.

In the metabasaltic rocks, the preservation of finely disseminated carbonate with $\delta^{13}C$ overlapping that of seafloor-altered protoliths, and the minimal mineralogical evidence of decarbonation, indicate large degrees of carbonate retention in this suite extending to UHP conditions similar to those beneath modern volcanic fronts. For many of the metabasalts, the $\delta^{18}O$ of this carbonate can be explained by closed-system equilibration with silicate phases (e.g., garnet, clinopyroxene) during HP/UHP metamorphism. Larger volumes of carbonate preserved in interpillow regions and as breccia-filling largely escaped decarbonation, showing little or no evidence for reaction with adjacent metabasalt. Calculated devolatilization histories demonstrate that, in a closed-system model, carbonate in metabasaltic rocks can largely be preserved to depths approaching those beneath volcanic fronts (80-90 km). Modeling of open-system behavior indicates that episodic infiltration of such rocks by H_2O-rich fluids would have greatly enhanced decarbonation. Trends in O-C isotope composition of carbonate in some metabasaltic suites likely reflect effects of infiltration by externally-derived fluid with or without resulting decarbonation. Carbonated ultramafic rocks similarly show little mineralogical evidence for decarbonation, consistent with calculated reaction histories, and have $\delta^{13}C$ largely overlapping that of seafloor equivalents. However, the high-grade ophicarbonates show more restricted ranges in $\delta^{18}O$ consistent with some control by infiltrating fluids, likely during subduction.

This combination of field, petrographic, and isotopic evidence, together with calculated decarbonation histories, is consistent with minimal loss of CO_2 from these rocks via decarbonation during forearc metamorphism. Combining our results with those of Cook-Kollars et al. (2014; *Chemical Geology*) for associated W. Alps metasedimentary rocks, we suggest that the majority of the CO_2 (perhaps 80-90%, considering the full range of rock types) could be

retained through forearcs in more intact volumes of subducting sediment, basalt, and ophicarbonate experiencing closed- or limited open-system conditions. Deep in forearcs and beneath arcs, decarbonation (and also carbonate dissolution) could be enhanced in shear zones and highly fractured volumes experiencing larger fluid flux in part from dehydrating sub-crustal ultramafic rocks in slabs. Degrees of C loss by decarbonation, carbonate dissolution, and partial melting should be particularly significant as the subducting sections experience heating to >600 ˚C at depths of 80-120 km (i.e., approximately at depths beneath arcs).

1. Introduction

Understanding of deep-Earth C flux in subducting oceanic lithosphere and sediments is crucial to modeling volatiles contributions to volcanic arcs, evolution of the atmosphere, and long-term degassing or regassing of the mantle (Berner et al., 1983; Berner, 1999; Zhang and Zindler, 1993; Marty and Toltskhin, 1998; Dasgupta and Hirschmann, 2010; Van Der Meer et al., 2014). Current understanding of the degrees of C retention to great depths in subduction zones is largely based on studies of volcanic gas output in comparison with subduction zone inputs, the latter based on knowledge of seafloor lithologies (see Hilton et al., 2002). Additional understanding has come from theoretical and experimental studies of phase stabilities in subducting oceanic lithologies (e.g., Kerrick and Connolly, 1998, 2001a,b; Molina and Poli, 2000; Gorman et al., 2006; Poli et al., 2009; Tsuno and Dasgupta, 2011; Schmidt and Poli, 2014; Cook-Kollars et al., 2014). There is general agreement that the behavior of C (and other major volatiles) along the subduction-zone metamorphic pathway must be taken into account when assessing long-term Earth degassing and atmosphere evolution (Bebout, 1995, 2007b, 2014; Javoy, 1998; Kerrick, 2001; Dasgupta and Hirschmann, 2010; Dasgupta, 2013; Cook-Kollars et al., 2014). However, there has been relatively little petrologic and geochemical study of decarbonation, and other mechanisms of C mobilization, in high-pressure (HP) and ultrahigh-

pressure (UHP) metamorphic suites representing the pathway taken by appropriate rock types subducting through forearcs and to beneath arcs.

A number of studies have considered global C subduction flux through comparison of subduction zone inputs in sediments, altered oceanic crust, and hydrated ultramafic rocks and subduction outputs in volcanic gases (e.g. Bebout 1995, 2007b, 2014; Hilton et al., 2002; Jarrard, 2003; Dasgupta and Hirschmann, 2010; Dasgupta, 2013). The complexity and related uncertainty of these estimates are evident in the large ranges of published input flux estimates presented in **Table 1** (also see Cook-Kollars et al., 2014). The combination of the uncertainties in the inputs and outputs results in a wide range in the estimates of volcanic arc return efficiency (16 - 80% arc return of the C entering trenches; **Table 1**). Some studies of arc volcanic CO_2 emissions have estimated the efficiencies of volcanic return of deeply subducted C for individual margins (e.g., Hilton et al., 2002; Shaw et al., 2003; Zimmer et al., 2004; de Leeuw et al., 2007; Marin-Ceron et al., 2010; Halldorsson et al., 2013). To examine the sourcing of C flux measured in volcanic gases, de Leeuw et al. (2007) compared C inputs measured by Li and Bebout (2005) for sediments outboard of the Central America trench. They suggested that contributions of sedimentary C alone could account for the measured output of gases and estimated a C return of 12-18% in Costa Rica and ~29% in El Salvador. The lack of a contribution of volatiles from subducting oceanic crust to arc volcanic gases was also suggested by Sano et al. (2001; Sano and Williams, 1996), Hilton et al. (2002), and Zimmer et al. (2004). However, it could be difficult to distinguish the contributions of CO_2 from carbonate sediment and from carbonate in altered oceanic crust based on the $CO_2/^3He$ and $\delta^{13}C$ of the volcanic gases (see House et al., 2014).

Theoretical studies have calculated phase stabilities for sediments, oceanic crust, and ultramafic lithologies associated with inputs into subduction zones (Molina and Poli, 2000;

Kerrick and Connolly, 1998, 2001a,b; Wei and Powell, 2003; Wei et al., 2003; Proyer, 2003; Connolly, 2005; Gorman et al., 2006; Cook-Kollars et al., 2014). Kerrick and Connolly (2001a) calculated mineral assemblages and volatiles concentrations for a wide range of sediment compositions, along subduction-zone *P-T* paths for modern margins, examining a closed-system model where decarbonation in subducting sediments allows CO_2 to be expelled from sediments without the influence of infiltrating, externally-derived H_2O fluids. In contrast, Gorman et al. (2006) investigated "open" system behavior in which crustal material, and sub-crustal slab ultramafic rocks, can contribute H_2O-rich fluids to overlying sediments and basalts, thus driving decarbonation reactions. It is conceivable that the H_2O-rich fluids emanating from the upper mantle in subducting slabs contain small amounts of CO_2 (or other C fluid species), depending on the C content of the hydrated ultramafic rocks (see Kerrick and Connolly, 1998; discussion by Alt et al., 2013). The coupling of external fluid-ingress and decarbonation within subducting slabs has been described in some studies of HP rocks (e.g., John et al., 2008; Ague and Nicolescu, 2014), and the opposite has also been described, with carbonation occurring along major intra-slab fluid conduits (Beinlich et al., 2010; John et al., 2012). Closed- and open-system scenarios can produce drastically differing degrees of forearc devolatilization (Gorman et al., 2006; see the discussion by Cook-Kollars et al., 2014), pointing to the need for "ground-truthing" by detailed study of devolatilization and fluid mobility in exposures of HP/UHP-metamorphosed oceanic lithologies.

Few studies have investigated the degrees of deep retention of C, as carbonate or reduced C (the latter largely metamorphosed organic matter), in appropriate lithologies (sediment, oceanic crust, and carbonated ultramafic rocks) and over the wide range of *P-T* conditions representative of trench to subarc metamorphism in subduction zones. The studies to date, mostly focusing on

metasedimentary suites, have indicated substantial retention of C and other volatiles during the relatively cool metamorphic conditions experienced at <40 km depths in most forearcs (see Bebout, 1995; Bebout and Fogel, 1992; Sadofsky and Bebout, 2003) and extending to depths approaching those beneath volcanic fronts (e.g., in the HP/UHP units in the Italian Alps; Cook-Kollars et al., 2014; also see Busigny et al., 2003; Bebout et al., 2013). Greater degrees of devolatilization and associated volatiles losses, including C isotope shifts in reduced C, occur in metasedimentary rocks along relatively warm subduction-zone *P-T* paths, such as those represented by the higher-grade units of the Catalina Schist (see Bebout, 1995; Bebout and Fogel, 1992). Other field and petrologic studies provide descriptions for UHP carbonate rocks at individual localities without detailed work evaluating extents of decarbonation and related isotopic shifts (e.g. Becker and Altherr, 1992; Kato et al., 1997; Zheng et al., 2003; Castelli et al., 2007; van der Straaten et al., 2008, 2012; Proyer et al., 2014; Lu et al., 2014). The smaller number of studies of HP/UHP metabasaltic rocks conducted at single localities, or over small ranges in grade (prehnite-pumpellyite to blueschist facies), have similarly indicated retention of C in subducting oceanic crust, with little or no isotopic shift, across metamorphic grades (Cartwright and Barnicoat, 1999, 2003; Miller et al., 2001). This points to the need for more thorough study of C loss from altered oceanic crust (AOC) and ultramafic rocks, the latter representing either peridotite hydrated and carbonated on the seafloor or sub-crustal slab ultramafic rocks hydrated and carbonated during slab bending and associated faulting and deep infiltration by seawater (see discussion of faulting and infiltration process by Ranero et al., 2005). The decarbonation and overall C loss history of deeply subducting AOC is particularly key to understanding subduction C cycling as this lithology could convey one-half to two-thirds of the subduction C input inventory into trenches (**Table 1**; see Dasgupta and Hirschmann, 2010;

Dasgupta, 2013; Cook-Kollars et al., 2014). The C subduction input in carbonated ultramafic rocks is likely far smaller, but still a significant flux (see Alt et al., 2013; **Table 1**).

In this study, we investigated the effects of prograde metamorphism, devolatilization, and other fluid-rock interactions on the retention and isotopic evolution of C in AOC and hydrated and carbonated ultramafic rocks that experienced HP/UHP metamorphism over a wide range of estimated peak temperatures and pressures (~0.2-3.0 GPa, 200-610°C). The work focused mostly on exposures in the Italian (and French) Alps, the Ligurian Alps, and the northern Apennines containing intact ophiolitic sequences and related cover sediments that experienced widely varying degrees of HP/UHP metamorphism (see **Fig. 1A**; geographic coordinates are provided in **Supplementary Table 1**). The rocks in the Western Alps are known to have experienced smaller amounts of exhumation-related overprinting than exposures of similar rocks in the Eastern and Central Alps and in most other HP/UHP metamorphic terrains around the world (Platt, 1986; Desmons et al., 1999a,b; Jolivet et al., 2003; Zheng, 2012), affording a more thorough assessment of prograde metamorphic devolatilization history (see Bebout, 2007a; Bebout et al., 2013). In this paper, we provide a smaller dataset for carbonate in veins, and as finely disseminated carbonate, in well-studied eclogites in the Tianshan, including eclogites sampled across the envelopes of veins interpreted to be significant intraslab fluid conduits and eclogites that were rehydrated to blueschist along the plate interface during their exhumation (Zack and John, 2007; van der Straaten et al., 2008, 2012; Beinlich et al., 2010; John et al., 2012). We integrate field and petrologic observations, theoretical calculations of devolatilization history (using the Perple_X software; Connolly, 2005), and O and C isotope data for these rocks, largely focusing on carbonate (and decarbonation history) but with some attention paid to the minor reduced C that could reside in the metabasalts. A companion paper (Cook-Kollars et al., 2014)

examined the record of devolatilization, and C release and mobility, in the metasedimentary rocks exposed at most of the localities in the Italian and French Alps investigated in our study (Cottian Alps and at Lago di Cignana).

2. Geologic Setting

The NW Italian and French Alps contain an abundance of Jurassic ophiolitic fragments that were formed ~160-170 Ma in the paleo-Tethys Ocean and rapidly subducted (~3 to 5 Ma) to peak metamorphic conditions ~45 Ma (Gebauer et al., 1997; Rubatto and Hermann, 2001, 2003). This region is of particular interest as it preserves slices of intact ophiolitic sequences metamorphosed over a wide range of peak *P-T* conditions (see **Fig. 1**), showing relatively small degrees of retrogression due to exhumation (Rubatto and Hermann, 2001; Parrish et al., 2006) and lithologically resembling modern Atlantic-type (slow-spreading rate) oceanic lithosphere (Lagabrielle and Cannat, 1990; Tricart and Lemoine, 1991; Cannat et al., 1997).

Internal Ligurides, Sestri Voltaggio Zone and Voltri Massif, Italy. Several units in the Internal Liguride units of the Northern Apennines, and of the blueschist to eclogite facies Sestri Voltaggio Zone and Voltri Massif, were sampled due to their exposure of ophiolitic sequences ranging from low-grade to HP conditions. Peak *P-T* conditions extend from 160-210°C at 0.2-0.3 GPa in the Bracco unit (Internal Liguride), 270-310°C at 0.6 GPa in the Mt. Figogna unit, and 300-350°C at 0.7 GPa in the Cravasco-Voltaggio unit (Leoni, et al., 1996), to ~550˚C at 2.0-2.5 GPa in Voltri. Several studies have investigated the fluid mobility and redistribution during the closed system retrogression of the high-pressure Voltri Massif (e.g., Vallis and Scambelluri, 1996; Scambelluri et al., 2004, 2007).

Ubaye Valley, France. Exposures at Pic du Pelvat in the Ubaye Valley, France, include ophicarbonates and relatively undeformed pillow basalts, with intact interstitial material. This crustal sequence is overlain by radiolarian chert and carbonate rocks (Tricart and Lemoine, 1986) and all rocks have experienced peak *P-T* conditions of 325-375°C and 1.1-1.4 GPa (Michard et al., 2004). This ophiolite fragment (with aerial exposure of about 1.5 km^2) was described by Tricart and Lemoine (1986) as an isolated megaboudin (slab) of oceanic crust retaining its original contact with the highly deformed Schistes Lustres metasedimentary section.

Monviso, Italy. The two tectonic slices of the Monviso ophiolite preserve eclogite-facies metamorphism at 480-515°C at 2.1 ± 0.3 GPa in the Monviso Unit and 520 to 570°C at 2.5 to 2.8 GPa in the Lago Superiore Unit (Angiboust et al., 2011, 2012). The metabasalt exposures of the Monviso unit vary greatly with some containing well-preserved carbonate-bearing pillow basalts and pillow breccias, and contain limited exposures of pelitic metasediments in contact with the metabasalts (also see Angiboust et al., 2012). The higher-grade Lago Superiore Unit contains rare exposures of relatively undeformed carbonate-bearing pillow basalts and pillow breccias with local intercalations of pelitic metasedimentary rocks.

Cervinia, Italy. The Zermatt-Saas ophiolite contains abundant pristine carbonate-bearing pillow basalts, pillow breccia, hydrothermalized basalts, and talc-schist serpentinites demonstrating little evidence of exhumation related retrogression (Ernst and Dal Piaz, 1978; Angiboust et al., 2009; Angiboust and Agard, 2010). In addition, exposures near Cervinia contain trench-fill pillow basalts, ranging from mm- to m-scale, that are cemented in a carbonate-dominated matrix. While the metamorphic grade of this region (520-560°C and 2.2-2.4 GPa; Angiboust et al., 2009) overlaps with that of Monviso, Servette, and Clavalité Valley, the dominance of carbonate in contact with well-preserved basalts, limited degree of retrogression, and the abundant garnet-

bearing rocks in the region are of interest in this study. Retention of oxidized and reduced C in the overlying metasedimentary rocks was investigated by Cook-Kollars et al. (2014).

Servette, St. Marcel and Clavalité Valleys, Italy (Zermatt-Saas). At this locality, exposures of pristine carbonate-bearing pillow basalts, pillow breccia, and hydrothermally altered basalts display chemical signatures of extensive seafloor alteration and contain abundant hydrothermal deposits (Martin and Tartarotti, 1989; Martin et al., 2008). These UHP eclogites contain pillow breccia with carbonate mineralogy varying from calcite to magnesite and often associated with chalcopyrite deposits. Peak *P-T* estimates (530-550°C at ~2.4 GPa), mapping, descriptions of the metabasalts, and some whole-rock chemical data are presented by Angiboust and Agard (2010).

Lago di Cignana, Italy. The UHP metabasalts of Lago di Cignana are the highest-grade rocks investigated in this study (van der Klauw et al., 1997; van der Klauw, 1998; see the petrologic study of the metasedimentary rocks at this locality by Reinecke, 1998). Recent studies have shown evidence of micro-diamond inclusions within garnets from these metabasalts and represent peak *P-T* paths of ~600°C and ≥3.2 GPa (Groppo et al., 2009; Frezzotti et al., 2011). Exposures of siliceous and carbonate/pelitic sediments associated with the pillow basalts have previously been studied for evidence of decarbonation (Cook-Kollars et al., 2014). Carbonate-bearing inter-pillow regions and veins are not abundant at this locality (see van der Klauw et al., 1997); however, small amounts of finely disseminated carbonate in whole-rocks afford an opportunity to investigate carbonate retention to depths approaching those beneath arcs.

Tianshan , China. Mafic HP rocks of the Tianshan Mountains in western China allow study of devolatilization along the blueschist- and eclogite-facies transition in seafloor-altered basalts metamorphosed at 480-580°C, 1.8-2.1 GPa and in some areas UHP conditions of 500-630°C and 2.4-3.3 GPa (see **Fig. 1B**; Klemd et al., 2002; Wei et al., 2003). The HP/UHP unit is interpreted

to reflect a tectonic mélange or accretionary wedge-like sequence, dominated by forearc sediments. Peak metamorphism occurred at ~315 Ma with the main exhumation processes at ~311 Ma (Klemd et al., 2005, 2011). Detailed field and chemical studies (e.g., Gao and Klemd, 2003; John et al., 2008, 2012) have yielded insights into the prograde dehydration of blueschist to carbonate-bearing eclogite veins and multiple textural carbonate setting within the basalts that have seen relatively little exhumation overprinting (Gao and Klemd, 2003; Klemd et al., 2005; Beinlich et al., 2010). van der Straaten et al. (2012) presented a small C and O isotope dataset for HP metabasalts from Tianshan which rehydrated to blueschists during their exhumation along the plate interface and suggested that the low $\delta^{13}C$ values of some of the carbonates reflect the influence of fluid from a source containing organic/reduced C.

3. Methods

3.1 Carbon and Oxygen Isotope Analyses

Carbonate from various textural settings (see **Table 2**) was sampled by micro-drilling using 1 and 2 mm tungsten carbide bits (data in **Supplementary Tables 2,3**). The samples were analyzed on a Finnigan MAT 252 using a GasBench II and methods described by Cook-Kollars et al. (2014). Carbonate mineralogy was assessed in part using a Hitachi TM-1000 scanning electron microscope (SEM) and carbonate other than calcite was observed only in metabasaltic samples from Zermatt-Saas (magnesite), Tianshan (ankerite; see van der Straaten et al., 2008, 2012), and Servette (magnesite in one sample suite), and some ophicarbonate samples (dolomite in La Pesca samples; magnesite in some Zermatt-Saas samples). For samples containing only a single carbonate phase, the calcite, dolomite, ankerite, or magnesite was reacted at 72°C for 0.5, 3, 3, or 6 hours (respectively) with 0.2 mL phosphoric acid to release CO_2. Bulk carbonate

analyses were performed on samples containing multiple carbonate phases, with the reaction time depending on the carbonate phases present. For a small number of samples, separate analyses of calcite and dolomite (by successive acid treatments exploiting the varying reaction rates and at varying temperatures) indicated very little difference in their isotopic compositions. Regular analysis of a house standard and international standard NBS-19 allowed monitoring and correction of the data, resulting in a standard deviation (1σ) of ~0.2‰ for both $\delta^{13}C$ and $\delta^{18}O$. The $\delta^{13}C$ and $\delta^{18}O$ values are reported relative to VPDB and VSMOW, respectively.

A small number of analyses of reduced C were obtained by first removing carbonate using 1N HCl. Samples were then oxidized in sealed 6 mm (o.d.) quartz tubes and combusted with Cu-CuO_x reagent before extraction and analysis by dual-inlet methods (methods in Li and Bebout, 2005). Accuracy was ensured by analyzing the graphite standard USGS-24, for which >50 analyses (over the last ten years) have yielded mean $\delta^{13}C$ of -16‰ with 1σ of <0.1‰. $\delta^{13}C$ is reported relative to VPDB.

3.2 Thermodynamic Modeling using Perple_X

Thermodynamic modeling was computed following the free-energy minimization approach using the software Perple_X (version 6.6.8, April 2013 version; Connolly, 2005) and the thermodynamic database of Holland and Powell (1998; with 2002 revision). Solution models (referred to as Do, Pheng, GlTrTsMr & GlTrTsPg, Gt, and Chl within the software) were used for carbonates, micas, amphiboles, garnet, and chlorite, respectively (Holland and Powell, 1998). Clinopyroxene stability was computed using the solution model by Gasparik (1989). Mineral end-member calculations for biotite, feldspar, and orthopyroxene were also considered but were not these phases were not stabilized at the selected *P-T* range and for the rock compositions investigated (compositions in **Supplementary Table 4**). The volatiles H_2O and CO_2 were

considered as thermodynamic components (not saturated phases) for the closed-system pseudosections and as saturated phases for the T-X_{CO_2} calculations. H_2O- and CO_2-bearing fluid behavior was modeled using the CORK equation of state by Holland and Powell (1991, 1998).

4. Results

4.1 Field Relations and Petrography

4.1.1 Metabasaltic Rocks

Generalized field textures and textural occurrences of carbonate at the sampling localities are presented in **Table 2**, with representative examples shown in the field photographs in **Fig. 2**. Most of the sampled exposures contain metabasaltic rocks showing little evidence for deformation at the macroscopic scale and containing clear pillow/interpillow structures and veins of varying textures, along with breccia, making it possible to sample carbonate from a variety of textural settings at single localities. Carbonate, mostly calcite, also occurs as a finely disseminated whole-rock phase and in relatively non-abundant micro- and macro-scopic scale veins and segregations. At the sites containing basaltic or gabbroic breccias, carbonate occurs as the dominant breccia filling (see **Fig. 2D**). Contacts of carbonate breccia fillings with metabasaltic clasts show no mineralogical evidence of metasomatic exchange — such metasomatism, had it occurred, might have driven some decarbonation (Thompson, 1975; Joesten, 1977; Ague and Rye, 1999; Bebout, 2013). Conspicuously absent in the W. Alps exposures are cm- to m-scale, through-going (i.e., at scales beyond those of individual small outcrops) veins indicating larger-scale fluid mobility (e.g., of the type described for Tianshan localities; see van der Straaten et al., 2008, 2012; Beinlich et al., 2010; John et al., 2012).

It is difficult petrographically to deduce mineralogical records of whole-rock decarbonation in the metabasalts, as the mineral assemblages are very similar to those expected as the result of HP/UHP metamorphism without any involvement of carbonate in prograde reactions. Calcium-rich phases that could in part reflect decarbonation of calcite or dolomite include garnet, omphacitic pyroxene, lawsonite, clinozoisite, as described in the previous petrologic studies of these localities cited in **Section 2** (discussion of this complication in **Sections 4.4 and 5.1.1**).

The carbonate sampled for this study, and analyzed for its C and O isotope compositions, is from a variety of textural settings (see **Table 2**, **Supplementary Table 2**). As noted in **Section 3.1**, for the metabasalts, carbonate other than calcite occurred only in samples from Zermatt-Saas (magnesite), Tianshan (ankerite; see van der Straaten et al., 2008, 2012), and Servette (magnesite in one sample suite). Many of the metabasaltic rocks contain 1-5 wt. % finely disseminated carbonate (as obtained from isotope extractions), in some cases not visible petrographically, but the dominant reservoirs for carbonate are in small-scale (<50 μm wide) veins of varying textures, breccia matrices, and interpillow regions. In some samples, μm to mm scale pods and veinlets are discontinuous beyond the scale of individual thin sections (several tens of mms), whereas others are through-going beyond this scale (up to cm and m scales) in rocks lacking penetrative deformation fabric. Some breccias contain >25% carbonate by volume (see the example in **Fig. 2D**), again, showing no obvious mineralogical evidence of reaction between the carbonate and the silicate mineral assemblages in the metabasaltic or metagabboic clasts.

4.1.2 Ultramafic Rocks (Ophicarbonates)

The ophicarbonate exposures sampled in this study, across all grades, are mostly breccias with variably metasomatized serpentinite clasts (cm to m scales) and extremely abundant carbonate as breccia filling and veins (together, up to 30 vol. % of some exposures) showing a

wide range of textures indicating their stages of evolution. At a few of the localities, the ophicarbonates show the development of later-stage, more penetrative cleavage, in some cases with intensely foliated rocks in which breccia textures are largely destroyed and nearby domains of non-foliated breccia, separated by deformation "fronts." The contacts between these highly deformed and undeformed ophicarbonates can be quite sharp, with strong gradients in extent of foliation over cm scales. The more foliated rocks tend to contain few veins cross-cutting their foliation. Although the majority of the ophicarbonates contain calcite as the dominant carbonate phase, samples from La Pesca contain abundant dolomite and some Zermatt-Saas samples contain magnesite.

4.2 Carbon and Oxygen Isotope Compositions of Carbonate (and Reduced Carbon) in Metabasaltic Rocks

Carbon and O isotope compositions for the metabasaltic rocks are shown in the compilation in **Fig. 3** (see **Supplementary Table 2** for textural occurrences of individual samples) and for individual sampling localities in **Fig. 4**. The carbonate occurrences at individual localities tend to show variation related to the textural setting of the carbonate, but there is significant overlap among the datasets for the various localities. Also shown in **Fig. 3** are ranges in C and O isotope compositions of finely disseminated (whole-rock) calcite in various altered basalts on the modern Atlantic seafloor (from Furnes et al., 2001) and data for calcite veins in seafloor-altered basalts (from Alt and Teagle, 2003; Coggon et al., 2010; R. Coggon, pers. comm., 2014). The data for the veins and finely disseminated carbonate in the metamorphic suites investigated here tend to show $\delta^{13}C$ similar to, but $\delta^{18}O$ lower than, values for carbonate from similar textural settings in basalts on the modern seafloor. However, the carbonate $\delta^{18}O$ values mostly fall within the range of whole-rock $\delta^{18}O$ values for altered oceanic crust (+5 to +20‰, mostly +5 to +10‰; from Alt

and Teagle, 2003; Alt, 2004). The carbonate $\delta^{18}O$ values for the Zermatt-Saas samples (~+9 to +20‰; green-filled symbols in **Fig. 3**) show a wide range encompassing the smaller ranges for the other units, among which there is more limited overlap.

Several suites demonstrate differences in values for whole-rock, including finely disseminated, carbonate and values for carbonate sampled from various other textural settings by micro-drilling (see **Fig. 4**). Carbonate in the lowest-grade (prehnite-pumpellyite facies) metabasalts, from the Bracco unit, have $\delta^{13}C$ of -4.5 to +2.0‰ and $\delta^{18}O$ values of +16 to +21.3‰ (see the previous work by Barrett and Friedrichsen, 1989). Except for several whole-rock samples (red-filled squares), the data for the Bracco Unit range in $\delta^{13}C$ values from -1.5 to +2.0‰ and show fairly uniform $\delta^{18}O$ of +16 to +17.3‰ (see **Fig. 4A**). Increasing in grade, discontinuous veins and pods in Mt. Figogna Unit metabasalts have $\delta^{13}C$ values of -0.2 to +0.8‰ and $\delta^{18}O$ values of +12.4 to +13.2‰, with one whole-rock sample having higher $\delta^{18}O$ near +17‰ (**Fig. 4A**). Approaching the blueschist facies, whole-rock analyses from the Cravasco-Voltaggio unit display $\delta^{13}C$ values of -2.6 to +0.8‰ and $\delta^{18}O$ values of +18.0 to +25.8‰ (see **Fig. 3**). Blueschist-facies metabasalts from Ubaye Valley, France, display large variation in whole-rock carbonate $\delta^{13}C$ of -12 to +0.3‰, correlated with $\delta^{18}O$ varying from +15.1 to +24.9‰ (see this trend in **Fig. 4C**). However, carbonate in discontinuous and through-going veins has $\delta^{13}C$ of -5.1 to +2‰ and shows tighter clustering in $\delta^{18}O$ of +14.0 to +16.9‰. Carbonate from various textural settings in rocks from the Lago Superiore unit at Monviso contain $\delta^{13}C$ values of -0.8 to +2.5‰ and $\delta^{18}O$ values of +8.5 to +15.9‰ (**Fig. 4B**). Through-going veins (green-filled diamonds) are relatively uniform in $\delta^{18}O$ (+11.5 to +12.5‰) and define a curved array between endmember $\delta^{13}C$ values of +2.5‰ and -0.8‰. The Monviso unit at Monviso contains carbonate with $\delta^{13}C$ of -0.4 to +1.2‰ however, with $\delta^{18}O$ values of +12.4 to +15.0‰ higher than those of

most Lago Superiore carbonate. Metabasalts from the Zermatt-Saas ophiolite show clustering of $\delta^{13}C$ values between -1.6 and +1.9‰ while having a broad range of $\delta^{18}O$ values of +9.1 to +19.2‰, showing little relationship with varying textures (**Fig. 4D**). The highest-grade metabasalts, at Lago di Cignana (UHP), display a wide range of whole-rock $\delta^{13}C$ values spanning from -6.1 to +0.7‰ and $\delta^{18}O$ values of +11.5 to +21.9‰, producing a linear array (red-filled squares in **Fig. 4D**).

Eclogites from the Tianshan show a wide range of carbonate $\delta^{13}C$, from -14.1 to +2.8‰, whereas $\delta^{18}O$ shows a smaller range of +9.9 to +15.8‰, and these data (for whole-rocks and discontinuous pods) form a strong trend (see the black arrow on the left in **Fig. 3**). These samples represent three traverses, one the envelope of a large vein (fluid conduit; see Zack and John, 2007) and the others of rocks partially rehydrated during fluid-rock interaction along the plate interface (see van der Straaten et al., 2008, 2012). For comparison, the data for metabasalts in the Catalina Schist (from Bebout, 1995) similarly show a range of $\delta^{13}C$ to values considerably lower than those expected for seafloor alteration, at relatively uniform $\delta^{18}O$. Among the sample suites for the localities in Italy and France, only Ubaye and Lago di Cignana show well-defined trends of covarying $\delta^{18}O$ and $\delta^{13}C$, in both cases toward higher $\delta^{18}O$ and lower $\delta^{13}C$ values approaching -15‰ (**Figs. 3, 4C,D**).

Several higher-grade metabasaltic samples were analyzed for their whole-rock C concentrations after pre-treatment with HCl (to dissolve carbonate), using the sealed-tube methods described in **Section 3.1**. Analyses of two Zermatt-Saas metabasaltic rocks yielded concentrations of 0.12 and 0.04 wt. % C with $\delta^{13}C$ of -22.4 and -26.7‰, respectively. One Monviso UHP metabasaltic rock yielded a C concentration of 0.07 wt. % (700 ppm) with $\delta^{13}C$ of -5.1‰.

4.3 Carbon and Oxygen Isotope Compositions of Carbonate in Ophicarbonates

Carbon and O isotope compositions of the carbonate in the ophicarbonates are shown in **Fig. 5** (see data in **Supplementary Table 3**), compared with the compositions of ophicarbonates from various settings, including the seafloor (the latter from Clerc et al., 2014). Most of the samples have $\delta^{13}C$ in the range of +0.3 to +3.0‰, but with the various suites show varying ranges and relationships in their $\delta^{18}O$. The highest-grade units (Voltri Massif, Zermatt-Saas) show the most tightly clustered and lowest $\delta^{18}O$ values (+9.9 to +12.6‰).

The prehnite-pumpellyite facies Bracco unit ophicarbonates show a range of $\delta^{13}C$ values of +0.6 to +2.8‰ and $\delta^{18}O$ values of +14.4 to +22.2‰, showing no obvious trends. Slightly increasing in grade, several samples of ophicarbonates from the Mt. Figogna unit tightly cluster in $\delta^{13}C$ (+0.7 to +1.2‰) and $\delta^{18}O$ (+14.0 to +14.9‰). Comparable in grade with Mt. Figogna, ophicarbonates from nearby Montaretto have $\delta^{13}C$ values of +1.0 to +2.6‰, however, show a broad range of $\delta^{18}O$ values from +15.1 to +24.6‰ (**Supplementary Table 3**; also see Schwarzenbach et al., 2013). Blueschist-facies ophicarbonates from Ubaye Valley, France, display the largest range in $\delta^{13}C$ values of the suites we investigated, spanning from -3.0 to +1.8‰ and $\delta^{18}O$ values of +16.0 to +25.4‰. Interestingly, the metabasaltic carbonate for Ubaye also shows this range to low $\delta^{13}C$ (see **Figs. 3, 4C**). Eclogite-facies ophicarbonates from the Zermatt-Saas ophiolite span a range in $\delta^{13}C$ values from -0.4 to +3.0‰ with a narrow range of $\delta^{18}O$ values (+9.9 to +12.6‰). Data for ophicarbonates from the Voltri Massif fall within the range of data for the Zermatt-Saas ophiolite, the other higher-grade (eclogite-facies) locality, with $\delta^{13}C$ values of +0.9 to +1.8‰ and $\delta^{18}O$ values of +10.1 to +11.3‰.

In general, the arrays of O and C isotope data for ophicarbonates and metabasalts from the same locality tend to overlap but show considerable differences in distribution (compare **Figs. 3**

and 4). For example, for the Bracco Unit, data for metabasalts show relatively uniform $\delta^{18}O$ of +16 to +17.5‰) and $\delta^{13}C$ ranging from -1.5 to 2.0‰. The ophicarbonates from the same locality have $\delta^{13}C$ of +0.5 to +3.0‰ and a show a wider range in $\delta^{18}O$ of ~+13.8 to +21.5‰. As another comparison, the Zermatt-Sass metabasalt carbonate ranges widely in $\delta^{18}O$, from +9 to +20‰, with $\delta^{13}C$ of -2.5 to +2‰. The ophicarbonate from the Zermatt-Saas shows a far more narrow range in $\delta^{18}O$ but $\delta^{13}C$ of -0.5 to +3.0‰ that largely overlaps the $\delta^{13}C$ range for the metabasalts.

4.4 Thermodynamic Modeling of the Devolatilization of the Metabasalts and Ophicarbonates

Pseudosections for four MORB compositions representing closed systems, generated using Perple_X, are shown in **Fig. 6** (the system modeled was NCKFMASH+CO_2; compositions are provided in **Supplementary Table 4**). The bulk compositions modeled in these calculations were selected to represent a wide range of alteration states and carbonate concentrations of seafloor-altered basaltic rocks (see Alt, 2004), with the composition for basalts at ODP Site 417/418 representing the most altered rocks. On these figures, dashed white lines represent an array of cool to warm modern-day subduction zone *P-T* paths from Syracuse et al. (2010) and van Keken et al. (2011; also P. van Keken, personal communication, 2013). The most significant changes in mineralogy, representing significant devolatilization, are shown with large dashed lines and arrows. For greater simplicity, minor oxide occurrences, as well as carbonate mineralogy, are excluded from the field labels. On these figures, the spectrum of colors represents CO_2 concentration and, on each, these concentrations show little change along lower-P, forearc parts of the *P-T* paths and significant decrease beginning at about 600˚C and at pressures of 2.0 to 2.75 GPa corresponding to 60-90 km depths (depending on the *P-T* path).

Figure 7 shows the calculated modal abundances of major silicate minerals and carbonates from the average composition of ODP core 417/418 (Staudigel et al., 1996) along the subduction

zone *P-T* paths for the four modern margins shown in **Fig. 6C** (paths from Syracuse et al., 2010; van Keken et al., 2011; P. van Keken, personal communication, 2013). To simplify the figure, minor mineral occurrences are omitted and carbonate mineralogy is indicated as an aggregate. Along each *P-T* path, garnet crystallization increases mostly at the expense of lawsonite. A decrease or loss of carbonates is coupled with the increase in clinopyroxene and to a lesser degree garnet. Glaucophane breakdown produces no changes in the modal abundances of major minerals or carbonates. Based on these variations in modal abundances, generalized reactions along these paths are likely to be of the following generalized types:

Reaction occurring prior to breakdown of carbonate:

glaucophane + garnet = clinopyroxene + H_2O (**Figs. 7A,B,C)** **(1)**

Reactions involving breakdown of carbonate:

lawsonite + clinopyroxene + carbonate = garnet + H_2O + CO_2 (**Figs. 7A,B**) **(2)**

garnet + carbonate = clinopyroxene + CO_2 (see **Figs. 7C,D**) **(3)**

Note that, for all *P-T* paths, lawsonite is produced prior to significant carbonate breakdown, thus presumably not via a decarbonation reaction. Glaucophane is not stabilized along the warmest *P-T* path, that for Cascadia (see **Fig. 7D**). Along all paths, beyond ~2.5 GPa, a bulk composition such as this (ODP Site 417/418) would stabilize a classic eclogite assemblage of clinoproxene+garnet largely devoid of volatiles, other than CO_2 in any residual carbonate, unless phases such as phengite are stabilized by small amounts of K_2O incorporated during seafloor alteration (see Bebout, 2007a). The superposition of these calculations and the various *P-T* paths show that, in the unlikely case where the released volatiles are still present (i.e., have not physically left the rock/system), some re-incorporation is possible at >3.0 GPa.

Figure 8A shows isopleths of H_2O and CO_2 for the closed-system model of the more altered rock composition from ODP core 417/418 (see **Figs. 6C,7**), the peak *P-T* estimates for the metabasaltic sites sampled in this study (shaded rectangular regions; see **Fig. 1B**), and the modern-day subduction *P-T* paths from **Fig. 6** (and also several *P-T* paths from Gerya et al., 2002; see the figure caption). Significant dehydration (~65%) is evident for the higher-grade suites studied here but little or no decarbonation is indicated for prograde metamorphism to these peak conditions. Along the *P-T* paths from Syracuse et al. (2010) for the various modern margins (thick grey lines), excluding the path for the very warm Cascadia margin, decarbonation reaction begins to occur at temperatures of ~600˚C and the maximum extents of decarbonation experienced by rocks along these paths are 7% for Tonga, 43% for Northern Vanuatu, and 100% for Nankai (the latter also a relatively warm margin). **Figure 8B** shows profiles of H_2O and CO_2 wt. %, plotted vs. pressure (and corresponding temperature), for a "cool" margin (Tonga), a margin "intermediate" in its *P-T* path (Northern Vanuatu), and a "warm" margin (Cascadia). On this figure, it is again clear that varying degrees of dehydration occur along earlier parts of these paths and to the peak-metamorphic *P-T* conditions for the units we sampled. As shown in **Fig. 7**, this H_2O loss is largely due to the breakdown of glaucophane and/or lawsonite giving way to clinopyroxene. More significant losses of CO_2 along the paths for Northern Vanuatu, Nankai, and Cascadia (see **Figs. 7B,C,D**) correspond to increase in the abundance of clinopyroxene.

The effect of infiltration by extremely H_2O rich fluids on mineral reaction for the composition representative of ODP Site 417/418 (from Staudigel et al., 1996) is demonstrated for two pressures (1.5 and 2.5 GPa) in the T-X_{CO_2} diagrams in **Fig. 9**. On these figures, carbonate is again simplified for clarity. **Figures 9A and B** present the same ranges in X_{CO_2} values at pressures of 1.5 and 2.5 GPa (respectively) and panels 1-4 below show the modal

abundances calculated for along pathways toward lower X_{CO_2} at two temperatures (450 and 550˚C) at each pressure (see the arrows pointing from higher to lower X_{CO_2}). As for the closed-system calculations, garnet crystallization occurs largely at the expense of lawsonite. The dramatic losses of carbonate are accompanied by large increase in clinopyroxene abundance and, at the higher temperature, also some increase in the abundance of garnet. In the calculation for 1.5 GPa and 550˚C, the decrease in the abundance of carbonate is more gradual than in the three other calculations and is accompanied by decrease in lawsonite abundance and increased abundance of garnet and, to a lesser extent, glaucophane.

Figure 10 shows a calculation of H_2O and CO_2 wt. % as a function of extents of devolatilization for an ophicarbonate composition and the *P-T* paths also shown in **Fig. 8A**. The peak *P-T* estimates for the ophicarbonates investigated in this study are shown as dark-shaded boxes and it is evident from this calculation that, in a closed system, little or no decarbonation would be expected. In the modern margins represented by the four *P-T* paths from Syracuse et al. (2010), modest amounts of decarbonation would be expected over the ~2.0 to 3.0 GPa interval.

5. Discussion of Results

Our integrated field, petrologic, theoretical, and geochemical approach allows a broad consideration of the extent to which C is retained in metabasaltic and metaultramafic rocks subducted to depths approaching those beneath arc volcanic fronts. Here, it is again worth noting that our work was conducted on large, relatively coherent/intact exposures of metabasaltic rocks and ophicarbonates, for the most part without obvious shear zones, and that with the exception of the Tianshan exposures we investigated, these exposures tended not to contain larger, more through-going vein sets indicative of open-system behavior.

5.1 Metabasaltic Rocks

5.1.1 Field Relations and Petrography of the Metabasaltic Rocks

Preservation of abundant carbonates in the relatively undeformed metabasalts, particularly in pillow/interpillow structures and pillow breccias, demonstrates the widespread retention of CO_2 (**Table 2**) in Italian/French Alps HP/UHP metabasalts subducted to depths of up to 90 km (**Fig. 2**). This evidence for the retention of carbonate is consistent with observations made in previous studies (e.g., Barnicoat and Cartwright, 1995; Rubatto et al., 1998; Cartwright and Barnicoat, 1999, 2003; Miller and Cartwright, 2000) and argues against the extensive decarbonation calculated for open-system models by Gorman et al. (2006). Unlike the larger, more through-going veins in the Tianshan (investigated by Beinlich et al., 2010; John et al., 2012; van der Straaten et al., 2012), which do show evidence for carbonate mobility, and the veins studied by Ague and Nicolescu (2014), the veins in the Italian exposures we investigated do not show obvious field or petrographic evidence of leaching or addition of carbonate in well-developed envelopes. However, it is possible that small amounts of carbonate were dissolved by infiltrating fluids, particularly from rocks showing evidence of control of their isotopic compositions from an external reservoir (e.g., metabasalts showing tight ranges in $\delta^{18}O$ or correlated shift in $\delta^{18}O$ and $\delta^{13}C$; see **Figs. 3,4**; see discussion of this possible open-system behavior in **Section 5.1.2**). Small amounts of carbonate dissolution, distributed over very large rock volumes, could constitute significant mobilization of C from or within slabs.

Petrographic/mineralogical identification of decarbonation in the HP/UHP metabasalts is made difficult by the fact that the mineral phases produced by such reactions are stabilized without the need for involvement of carbonates (see the calculations in **Fig. 6** for basalts containing a wide range of initial CO_2 concentrations). However, for a small number of samples,

from Ubaye and Tianshan, possible evidence of decarbonation occurs as reaction rims at contacts between mafic breccia clasts and carbonate cement. Within pillow matrices, across the wide-range of *P-T* represented by our localities, carbonate is predominantly finely disseminated and displays little evidence of reaction with surrounding silicates to produce calc-silicate phases and release CO_2. In a small number of metabasalts, discontinuous carbonate-bearing veins show reaction rims with amphibole, epidote, and omphacite, pointing to local-scale metasomatic reaction possibly involving CO_2. The surprisingly small number of through-going carbonate-bearing veins in these relatively undeformed metabasaltic exposures (most of them preserving pillow textures; see **Table 2**; **Figs. 2A-C**) is consistent with limited degrees of large-scale fracture-related fluid-flow (i.e., fluid mobility at scales greater than the individual outcrops).

5.1.2 Isotopic Evidence for Closed to Limited Open-System Behavior during Subduction-Zone Metamorphism of the Metabasaltic Rocks

The C and O isotope data for the metabasalts (see **Figs. 3,4**) allow some assessments of extents of open- and closed-system behavior and, where open-system behavior is indicated, the compositions and possible sources of the externally-derived fluids. In this discussion of the isotopic data, we do not consider in detail the consequences of having minor amounts of dolomite, ankerite, or siderite in some samples, in addition to the far more abundant calcite. Fractionation of C (and O) isotopes among these phases is minor, near 0.5‰ ($10^3 \ln\alpha$), over the temperature range of 400-600˚C (see Sheppard and Schwarz, 1970).

The majority of the suites retain carbonate $\delta^{13}C$ overlapping with that of carbonates produced during seafloor alteration; however, the $\delta^{18}O$ values are significantly lower than those for the seafloor carbonates (see **Figs. 3, 4**). Although shifts to lower $\delta^{18}O$ could be accomplished through open-system behavior, involving infiltration by fluids from external sources, we suggest

that (particularly for the finely disseminated carbonate, micro-veins, and segregations) these shifts could be the result of more closed-system exchange between the carbonate and the modally dominant silicate mineral assemblage. Calculation of equilibration of calcite $\delta^{18}O$ with clinopyroxene and garnet, at 500-600˚C, in a fictive eclogite with whole-rock $\delta^{18}O$ of +10‰ (using fractionation factors from Zheng, 1993) yields values near +13‰ within the range of observed values for the finely disseminated carbonate (see **Fig. 3**). A number of other authors have concluded that HP/UHP metabasaltic rocks can behave largely as closed systems during metamorphism, based in part on O isotope compositions (see Barnicoat and Cartwright, 1995; Cartwright and Barnicoat, 1999, 2003; Miller et al., 2001; Nadeau et al., 1993; Philippot, 1993).

Decarbonation involving finely disseminated calcite in the metabasalts would be expected to produce lowering of $\delta^{13}C$, with or without change in $\delta^{18}O$, the O shifts depending on the extents to which the decarbonation is driven by infiltration by externally-derived H_2O-rich fluids (and the $\delta^{18}O$ of these fluids). For the closed-system case, with no infiltration, decreases in $\delta^{18}O$ due to decarbonation are strongly limited by the relatively small fractions of O removed in the CO_2 (i.e., the large fraction of O left in the residue in silicate phases and any residual carbonate). For extensive decarbonation of finely disseminated carbonate, where the fraction of C remaining can approach or reach 0, shifts of up to 10‰ or greater are possible by a Rayleigh distillation process (see Valley, 1986). One representative path in O-C isotope composition that residual carbonate might take for a Rayleigh process is shown in **Fig. 3**. It would be difficult to identify the small shifts in $\delta^{18}O$ potentially associated with closed-system decarbonation, given the very large range of possible starting $\delta^{18}O$ values related to seafloor alteration (see Alt et al., 1996; Alt and Teagle, 2003; Furnes et al., 2001) and the superimposed exchange with silicate phases. However, the lack of shift of $\delta^{13}C$ to beyond the range expected for seafloor-altered basalts, observed for most

of the metabasaltic suites, is consistent with little or no decarbonation. For the case of an infiltrating extremely C-poor, H_2O-rich fluid driving decarbonation reaction, any $\delta^{13}C$ shift would be purely the result of decarbonation, and the exact direction and magnitude of $\delta^{18}O$ shift would depend on the $\delta^{18}O$ of the fluid and the temperature at which the residual carbonate equilibrated with that fluid (see the double-headed arrow near the top of **Fig. 3** labeled, "Exchange with H_2O-Rich Fluid").

For a few of the suites, isotopic compositions are indicative of some open-system behavior and, in some cases, consistent with equilibration with fluids derived in nearby metasedimentary rocks (see the data for these metasedimentary sections in Cook-Kollars et al., 2014). The relatively uniform $\delta^{18}O$ for veins in the low-grade Bracco Unit (**Fig. 4A**) indicates the possibility of some control of isotopic compositions by exchange with an externally-derived fluid with relatively uniform $\delta^{18}O$ but that did not result in $\delta^{13}C$ differing from that typical for seafloor altered basalts (compare with the ranges of $\delta^{13}C$ in **Fig. 3**). Some whole-rock carbonate in these metabasalts (red-filled squares) is considerably higher in $\delta^{18}O$ and shows a wide range of $\delta^{13}C$ values, perhaps reflecting differential control by infiltrating fluids and greater preservation of isotopic compositions inherited from the seafloor or influenced by some decarbonation (the latter producing shift to lower $\delta^{13}C$ values). Whole-rock, finely disseminated carbonate in blueschist metabasalts from the Ubaye Valley shows shifts towards more organic-rich $\delta^{13}C$ signatures (**Fig. 4C**), perhaps in part reflecting decarbonation or isotopic exchange with minor reduced C in these samples, and correlated shift to higher $\delta^{18}O$. These shifts could reflect exchange with externally-derived, C-bearing, H_2O-rich fluids, with or without some shift associated with decarbonation. Similar relationships are exhibited by whole-rock data for very low-carbonate UHP metabasalts from Lago di Cignana. Data for more through-going veins in the Lago Superiore Unit at

Monviso (green-filled diamonds in **Fig. 4B**) show a modest range of $\delta^{13}C$ but a very narrow range of $\delta^{18}O$, the latter perhaps reflecting control of O isotope composition by fluids with uniform $\delta^{18}O$ from an external source. The range in $\delta^{13}C$ of these Lago Superiore veins (note the varying y-axis ranges in $\delta^{13}C$ in the plots in **Fig. 4**) contrasts with the far larger ranges in $\delta^{13}C$, also at fairly uniform $\delta^{18}O$, seen for the Tianshan and Catalina Schist metabasalts (see **Fig. 3**). The data for these latter two suites could reflect exchange with fluids with uniform $\delta^{18}O$ but that previously equilibrated differentially with organic-rich sediments during entrainment into a shear zone (for some samples, perhaps with some superimposed isotopic effects of decarbonation; for discussion of the Catalina Schist data, see Bebout, 1995).

For some of the Alps suites, the $\delta^{18}O$ of calcite showing relatively narrow ranges, without appreciable shift in $\delta^{13}C$ from the range for altered seafloor basalts, differs significantly from the calcite $\delta^{18}O$ values in nearby calc-schists of similar grade that could perhaps be viewed as potential fluid sources. The best examples of this relationship are the subset of MV-LS samples showing more through-going textures (green-filled diamonds in **Fig. 4B**; $\delta^{18}O$ near +12‰) and data for various vein types at the Bracco Unit localities ($\delta^{18}O$ near +16.5‰). Neither of these isotopic compositions is consistent with equilibration with carbonate from the calc-schists (via fluids), which at these grades has $\delta^{18}O$ near +18‰ (Monviso) and +25‰ (estimated for Bracco; see Cook-Kollars et al., 2014). The lower-$\delta^{18}O$ fluids producing these arrays could have been largely from another source such as dehydrating mafic or ultramafic rocks at greater depths in the subduction zone, perhaps with some in-mixing of fluids evolved in the calc-schist/metapelite section. The trends toward higher $\delta^{18}O$ and lower $\delta^{13}C$ for some of the samples from the Ubaye Unit and the Zermatt-Saas localities (the gray-shaded diagonal arrow in **Fig. 3**) are consistent

with a shift toward equilibrium with fluids equilibrated with interlayered calc-schists and metapelites of the Schistes Lustres exposed nearby.

5.1.3 Theoretical Evidence for Decarbonation History of the Deeply Subducted Metabasalts

The thermodynamic calculations for closed systems presented in this paper, and by Kerrick and Connolly (2001b), indicate that very little decarbonation would occur at forearc depths along the *P-T* metamorphic gradient investigated in this study (and by Cook-Kollars et al., 2014), and along forearc *P-T* paths experienced in most modern subduction margins. For the compositions considered in this study, and by Gorman et al. (2006), significant decarbonation occurs only at very low X_{CO_2}, a condition that seemingly would require infiltration of the rocks by H_2O-rich fluids (see **Fig. 9**). For depths greater than those investigated in these field localities (i.e., >90 km), even the closed-system calculations indicate significant decarbonation, depending on the *P-T* path the rocks experience (**Figs. 6, 8**). Use of the more recently published *P-T* paths (Syracuse et al., 2010; van Keken et al., 2011) produces far larger CO_2 loss over the depth interval of 80-120 km than was suggested by Kerrick (2001a,b), who considered earlier models that did not take into account the heating of slabs by the convecting mantle wedge.

These calculations for the metabasaltic rocks would permit infiltration of the metabasalts by fluids that were H_2O-rich (i.e., had high O/C) but had X_{CO_2} higher than that required to drive decarbonation reaction. This scenario would conceivably produce shifts in carbonate $\delta^{18}O$ without as obvious shifts in $\delta^{13}C$ (see the arrow in **Fig. 3** labeled "Exchange with H_2O-Rich Fluid"), depending on the $\delta^{18}O$ of the fluid, the temperature of equilibration, and to a lesser extent, the carbonate mineralogy. Some of the metabasaltic suites, particularly Ubaye and Cignana (see **Figs. 3,4**), could have been shifted to higher $\delta^{18}O$ and lower $\delta^{13}C$ by a C-bearing infiltrating fluid with X_{CO_2} insufficiently low to drive decarbonation reaction (see **Fig. 9**). As

noted in **Section 5.1.2**, for many of the metabasalts, the shifts in $\delta^{18}O$ of whole-rock carbonate (finely disseminated and in small pods and discontinuous veinlets) are consistent with isotopic exchange of the carbonate with the more abundant silicate phases in these rocks, thus seemingly requiring no influence by externally-derived fluids.

5.2 Metaultramafic Rocks

The highly carbonated metaultramafic rocks (ophicarbonates) investigated here show little or no mineralogical evidence of decarbonation, consistent with the theoretical calculations of Kerrick and Connolly (1998), and in **Fig. 10**, for prograde reaction in closed systems. Field and petrographic study demonstrates retention of carbonate, for example, with little to no evidence of reaction of carbonate with ultramafic clasts at macro- and micro-scopic scales. In a number of the ophicarbonate exposures, the lack of foliation, retention of breccia cement textures resembling those produced by seafloor alteration, and lack of more through-going veins are consistent with a lack of larger-scale carbonate mobility during subduction. The localization of any subduction-zone deformation along discrete shear zones allows preservation of original breccia textures in more intact and undeformed zones, and the isotopic compositions of these features overlap with those of ophicarbonate produced on the seafloor (see **Fig. 5**; cf. Schwarzenbach et al., 2013). The wide range of C and O isotope compositions for seafloor ophicarbonate (the protoliths) complicates identification of change due to subduction zone metamorphism. However, with the possible exception of the data for the Voltri-Massif and Ubaye, the $\delta^{13}C$ values do not show obvious evidence for decarbonation (see the typical Rayleigh trend for decarbonation in **Fig. 3**), supporting the mineralogical evidence for a lack of such reaction. As for some of the metabasalts (e.g., Monviso; see **Fig. 4B)**, the highest-grade ophicarbonates (particularly Zermatt-Saas and Voltri-Massif) show relatively narrow ranges in

$\delta^{18}O$ that could reflect the influence of a fluid from an external source. Lowering of the $\delta^{13}C$ of some samples in these suites, particularly Ubaye, hints at either a decarbonation effect or the influence of organic C in the fluid source, perhaps via exchange with nearby metasedimentary rocks (as for metabasalts from the same locality; see **Figs. 3,4C**). Ophicarbonates from the lower-grade suites (Bracco, Mt. Fignona, and Ubaye) show wide ranges in $\delta^{18}O$ perhaps consistent with greater preservation of seafloor alteration signatures. Combining the field, petrographic, isotopic and theoretical evidence, it appears that the ophicarbonates behaved as relatively closed systems, at the high grades perhaps with some episodic infiltration by fluids from external sources insufficient to drive appreciable decarbonation. This implies that a large fraction of the carbonate incorporated into such rocks at/near the seafloor can be retained to great depths in subduction zones, perhaps to 80-90 km.

Comparison of our calculations for ophicarbonates with those of Kerrick and Connolly (1998) demonstrates the strong dependence of calculated decarbonation on the rock composition employed in the calculations. Both the calculations in **Fig. 10** and by Kerrick and Connolly (1998) indicate that such rocks would largely retain carbonate when subducted along a forearc *P-T* gradient such as that represented by our HP/UHP rocks and experienced in many modern subduction zones (example *P-T* paths shown in **Fig. 10**). However, the further heating at the top of the slab and sediments (to >600 ˚C) at 80-120 km depths (see **Fig. 10**) could result in appreciable decarbonation and the calculations by Kerrick and Connolly (1998) show more dramatic loss of CO_2 during this heating than demonstrated in our calculations in **Fig. 10**. For the composition modeled in Fig. 1A of Kerrick and Connolly (1998), nearly 100% loss of CO_2 would be predicted along a *P-T* path similar to that for N. Vanuatu.

5.3 Implications for Deep Subduction-Zone Carbon Cycling

In this study, as in the studies by Bebout et al. (2013) and Cook-Kollars et al. (2014), focus is placed on understanding devolatilization history of relatively "intact" volumes of lithologies thought to be subducting into modern margins. These exposures contain few through-going, larger vein networks and, for the most part, the metabasalts and ophicarbonates do not show the development of penetrative deformation textures (e.g., containing intact pillow structures). All suggestions are that intact slabs and sediment sections would tend to behave as relatively closed systems except along the more extensive fracture networks and in other particularly deformed zones (e.g., shear zones) that would channelize dehydration-related fluid release (e.g., Zack and John, 2007; John et al., 2012; Konrad-Schmolke and Halama, 2014; Fusseis et al., 2009).

A number of authors have proposed relatively closed-system behavior during prograde metamorphism of less-deformed tracts of HP/UHP metabasaltic rocks and many of these studies were focused on metabasalts in the European Alps. Philippot and Selverstone (1991), Barnicoat and Cartwright (1995), Cartwright and Barnicoat (1999), Spandler et al. (2011; these authors suggested some limited open-system behavior), Nadeau et al. (1993), Widmer and Thompson (2001), and Rubatto and Hermann (2003) all invoked relatively local-scale control over fluid composition and little infiltration of mafic meta-ophiolitic rocks by externally-derived fluids (see the discussion by Scambelluri and Philippot, 2001). More recently, Angiboust et al. (2011; 2014) have identified brecciated and sheared domains, within large intact volumes of the Monviso Massif, that likely represent channelways for fluids transported over longer distances. Longer-distance fluid flow through localized fluid conduits in coherent slab sections and at the subduction interface has been proposed for a number of other HP/UHP localities (e.g., Herms et al., 2012, Ecuador; John and Schenk, 2003, Zambia; Gao et al., 2007, Beinlich et al., 2010, John et al., 2012, and Li et al., 2014, Tianshan; Spandler and Hermann, 2006, New Caledonia;

Breeding et al., 2004; Miller et al., 2009, Cyclades; Ague and Nicolescu, 2014, Corsica). This proposed focusing of fluid flow (and related metasomatic alteration) in highly sheared and fractured zones echoes conclusions from study of the Catalina Schist (California), in which metasomatism and isotopic homogenization was enhanced in such zones (Bebout, 1991; Bebout and Barton, 1993; King et al., 2006, 2007) and larger volumes of less permeable, less-deformed metasedimentary and metamafic rock behaved as systems closed to infiltration by externally-derived fluids (Bebout and Fogel, 1992). The extent to which enhanced C loss along these more strongly deformed zones contributes to the overall C flux from subducting top-slab sections requires further field investigation. The studies of C mobility along such structures have tended to be conducted on individual or small numbers of exposures and an assessment of the broader significance of such loss will need to be conducted on a more regional scale.

Very simply considered, a loss of 10% of initially subducted C to forearc devolatilization reactions implies delivery of 90% of this C inventory to depths beneath arcs (global average of 105 km; Syracuse and Abers, 2006), where another fraction could be extracted to contribute to arc CO_2 degassing and other forearc and mantle wedge C reservoirs. Loss of another 40% of the C beneath arcs would imply that 50% of the C could be contributing to mantle regassing on modern Earth. However, this simple comparison overlooks the likely inefficient delivery of any CO_2 released from subducting slabs into arc source regions and ultimate return of this CO_2 to the atmosphere. Considerable amounts of C could be transported updip toward the seafloor, along the subduction thrust, or stored in the forearc or subarc mantle wedge.

Table 3 provides estimates of extents of closed-system CO_2 loss, due to decarbonation reactions, as rocks traverse the 80-120 km depth range over which further heating occurs (to >600˚C). These losses are based on the thermodynamic calculations in **Figs. 6-8 and 10** (for

metabasaltic rocks and ophicarbonates) and the calculated *P-T* paths from Syracuse et al. (2010) for the top of the slab in selected modern Earth subduction zones (Cascadia, Nankai, Northern Vanuatu, and Tonga). Cook-Kollars et al. (2014; see their Supplementary Fig. 3) similarly superimposed these thermal models on the closed-system calculations of Kerrick and Connolly (2001a) for a range of sedimentary compositions from Plank and Langmuir (1998).

The estimates of CO_2 loss in **Table 3** demonstrate the strong, expected relationship between extents of deep volatiles cycling and subduction-zone thermal structure, the latter related to a number of physical and thermal factors (see discussions of the more recent thermal models by Syracuse et al., 2010; van Keken et al., 2011). For the closed-system model, extensive (perhaps complete) CO_2 loss is expected to occur in carbonated basalt and the more mixed clastic-carbonate sediment sections (for the latter, GLOSS and Antilles), whereas ophicarbonate and the more pure carbonate sections (Marianas, Vanuatu) could retain large fractions of their CO_2 over this depth range. Here, it is important to recall that subducting altered oceanic crust is believed to convey one-half to two-thirds of the C entering trenches, on a global basis (see **Table 1**). The same metabasaltic composition (417A-24) could lose as little as 7% of its CO_2 traversing this same depth range in the very "cool" Tonga margin. It is unlikely that the endmember closed-system modeling truly approximates decarbonation history at depth in subduction zones, as the limited, evolving permeability of the intact volumes of rocks will afford some pervasive infiltration, and fracture networks are likely to greatly enhance access to the carbonate-bearing sections by H_2O-rich fluids derived elsewhere in the subducting sediment and ophiolitic section (see **Fig. 9**). Also uncertain is the role of partial melting of various subducting lithologies in mobilizing C beneath arcs (van Keken et al., 2011; Tsuno et al., 2012; discussion by Dasgupta,

2013). Thus, the estimates of CO_2 loss in **Table 3** provide a crude assessment of the *minimum* losses expected for such rocks.

An assessment of whether closed-system to limited open-system behavior, as demonstrated here, can result in decarbonation sufficient to balance arc CO_2 outputs is further complicated by the poor constraints on volcanic CO_2 flux in many individual arcs (see the review by Hilton et al., 2002). The most detailed attempt to match subduction C inputs with arc volcanic gas outputs was that of de Leeuw et al. (2007), who suggested that C contributions from the sediments alone could account for the measured output of gases and estimated a sedimentary C return of 12-18% in Costa Rica and ~29% in El Salvador (i.e., with no contribution of C from the subducting oceanic crust). The calculated CO_2 losses in **Table 3**, for subduction along moderately warm *P-T* paths such as those at the Central America margin (for Costa Rica and Columbia/El Salvador, very similar to the path for N. Vanuatu; van Keken et al., 2011), are consistent with the proposed CO_2 returns from subducting sediments in that margin (12-29%), depending on the exact proportions in that margin of mixed carbonate-clastic sediments undergoing reaction. Interestingly, a slightly larger return of sedimentary CO_2 is estimated for the El Salvador margin for which the *P-T* path is somewhat warmer than that for Costa Rica. However, de Leeuw et al. (2007) provide a discussion of the full range of factors that could control these arc volcanic returns.

In addition to decarbonation (and possibly, partial melting), carbonate dissolution, discussed by Ague and Nicolescu (2014; see Caciagli and Manning, 2003; Manning et al., 2013; Manning, 2014; cf. John et al., 2008), Frezzotti et al. (2011), and Facq et al. (2014), and conceivably also carbonate reduction (Galvez et al., 2013; Lazar et al., 2014), could mobilize C from slabs, particularly in regions experiencing significant fluid flux (more densely fractured rock volumes,

shear zones). Greater understanding of the significance of these processes in contributing to C flux from subducting slab+sediment sections also awaits further field and geochemical investigation. Further confounding any quantitative assessment of C flux from these sections, regardless of the mechanism, is the observation that C can also be *enriched/deposited* in some sites, for example, in veins and their envelopes (as both carbonate and graphite; see Bebout, 1995; Gao et al., 2007; Beinlich et al., 2010). In this scenario, C is redistributed within subducting slabs and evolving subduction interfaces, but not necessarily removed from these domains and available for addition to the overlying mantle wedge. At shallower levels of forearcs (<40 km), particularly in paleoaccretionary complexes, this C "capture" is demonstrated by the voluminous carbonate veining and, to a lesser extent, deposition of graphite in veins (see Bebout and Barton, 1993; Bebout, 1995; Sadofsky and Bebout, 2003).

A number of other factors can be envisioned as important in dictating C losses at individual margins, beyond the varying thermal structures, types of sediments, and extents of carbonation in subducting slabs on which we focus in this paper. The thickness of the upper lithospheric plate dictates the depths at which the tops of subducting slabs are heated by exposure to the convecting mantle wedge. Structural state of the incoming oceanic crustal section, and related degrees of seafloor alteration, can be strongly affected by the rates of spreading, with oceanic crust produced by slow spreading (e.g., Atlantic type) tending to be more hydrothermally altered and with gabbros and ultramafic rocks exposed to seawater by large-scale extensional faulting. In the Atlantic Ocean, hydrated and carbonated ultramafic rocks have been recovered by dredging and are believed to be abundant on the modern seafloor (Cannat et al., 1997). As another factor, CO_2 contents in oceanic basement can vary with the age of the basement, for example, with Mesozoic basement containing more CO_2 than Cenozoic basement reflecting varying atmospheric CO_2

levels (see Alt et al., 2013, and references therein). Finally, modern margins show varying degrees of subduction accretion and erosion (Scholl and von Huene, 2010), in some cases varying along individual margins, and such processes could strongly influence (1) the extent to which parts of the initially subducted sediment section are subducted into the deep forearc and to beneath arcs, and (2) whether large amounts of C-bearing forearc material are entrained to great depths by removal from the hanging wall.

6. Conclusions and Outlook

Following are some conclusions reached in this integrated field, petrologic, and geochemical study and several comments regarding some directions that could be taken in further investigation of metamorphic C fluxes in subduction zones.

— Combining our results with those of Cook-Kollars et al. (2014), it appears that intact volumes of forearc-metamorphosed metabasaltic, meta-ultramafic, and metasedimentary rocks, away from zones of more intense deformation (shear zones, dense fracture networks with through-going veins), could experience only minor amounts of decarbonation, retaining unreacted carbonate with varying textures during prograde metamorphism to depths approaching those beneath volcanic fronts. In metabasalts, the majority of this carbonate likely resides in interpillow regions and breccia matrices, as has been observed for altered oceanic crust recovered during deep-sea drilling (see Gillis and Coogan, 2011). Loss in forearcs of CO_2 from ophicarbonates also appears minor based on combination of field results with modeling and isotopic study.

— Rocks of these compositions could experience far larger amounts of decarbonation if infiltrated by H_2O-rich fluids (consistent with the modeling results of Kerrick and

Connolly, 1998, 2001a,b; Connolly, 2005; Gorman et al., 2006). Taking into account the effects of limited open-system behavior, and matching Perple_X calculations with observed changes in mineral modes, Cook-Kollars et al. (2014) estimated 10-20% loss of CO_2 from the Schistes Lustres/Cignana metasedimentary section. Shifts in $\delta^{18}O$ in some metabasalts, correlated with decrease in $\delta^{13}C$, and extremely uniform $\delta^{18}O$ in other suites, could reflect infiltration by H_2O-rich fluids (containing minor C species) from external sources.

— Decarbonation, and also carbonate dissolution, is probably enhanced in shear zones and more dense networks of larger-scale veins — the amount of such loss could be significant along major pathways of slab fluid release or disrupted subduction interfaces at which disparate lithologies are juxtaposed and experience interaction with large amounts of fluid (see Bebout and Penniston-Dorland, 2014, in review). Further field-based work should be aimed at assessing extents of loss of volatiles along such structures, the mechanisms of loss (e.g., decarbonation, carbonate dissolution, in part related to fluid influx or mixing; see John et al., 2008; Poli et al., 2009), and whether this loss can contribute significantly to the overall C flux from subducting slab+sediment sections.

— Organic C is estimated as representing ~20% of the subduction C input inventory (Agrinier et al., 1985; Bebout, 2007b). Although the delivery of this reduced C reservoir into subduction zones is expected to be dominantly in sediments, there is some suggestion that deeply subducting metabasaltic rocks could contain significant amounts of reduced C (see **Section 4.2**) that should be considered in assessments of deep C subduction. Of the three whole-rock analyses of reduced C presented in this paper, two resemble organic C in their $\delta^{13}C$ (near -25‰), and the third resembles the upper mantle, near -5‰.

— The increased heating of subducting slabs and sediments (to >600 ˚C) over the approximate depth interval of 80-120 km (see the *P-T* paths from Syracuse et al., 2010, and Gerya et al., 2002, in **Figs. 6,8A,10**) could enhance decarbonation and dissolution and potentially lead to partial melting (van Keken et al., 2011; Tsuno et al., 2012; discussion by Dasgupta, 2013), conceivably resulting in release of C in quantities sufficient to balance arc outputs.

— Return of slab-released C to the atmosphere in volcanic arc gases could be quite inefficient — large amounts of C could be stored in the forearc and in the subarc mantle wedge. Greater understanding of this storage is necessary for estimates of the proportion of initially subducted C entering the deeper mantle (i.e., surviving to depths beyond subarc regions).

— Our work points to the need to investigate C cycling at individual margins with well-known physical characteristics, including subduction inputs, and thermal structure. Such work might best be done on individual margins for which such parameters are known to vary along strike, providing an analysis of the most important forcing factors (see de Leeuw et al., 2007; House et al., 2014).

Acknowledgements

Funding for this project came mostly from National Science Foundation grant EAR-1119264 (to GEB). We extend special thanks to James Connolly for his helpful comments and assistance with the use of the Perple_X software, and to Peter van Keken for providing updated calculated *P-T* paths for modern subduction margins. Rosalind Coggon kindly provided a compilation of the O and C isotope compositions of veins in seafloor basalts. MS acknowledges funding from the Italian MIUR (PRIN-COFIN project 2012R33ECR_002). We thank Jeff Alt and an anonymous reviewer for their constructive and useful comments and suggestions.

References

Agrinier, P., Javoy, M., Smith, D.C., Pineau, F., 1985. Carbon and oxygen isotopes in eclogites, amphibolites, veins and marbles from the Western Gneiss region, Norway. Chem. Geol. 52, 145-162.

Ague, J.J., Nicolescu, S., 2014. Carbon dioxide released from subduction zones by fluid-mediated reactions. Nature Geosci., DOI: 10.1038/NGEO2143.

Ague, J.J., Rye, D.M., 1999. Simple models of CO_2 release from metacarbonates with implications for interpretation of directions and magnitudes of fluid flow in the deep crust. Jour. Petrol. 40, 1443-1462.

Alt, J.C., 2004. 15. Alteration of the upper oceanic crust: mineralogy, chemistry, and processes. in Davis, E.E., Elderfield, H., Hydrogeology of the Oceanic Lithosphere, Cambridge University Press, pp. 497-535.

Alt, J.C., Laverne, C., Vanko, D.A., Tartarotti, P., Teagle, D.A., Bach, W., Wilkens, R.H., 1996. Hydrothermal alteration of a section of upper oceanic crust in the eastern equatorial Pacific: A synthesis of results from Site 504 (DSDP Legs 69, 70, and 83, and ODP Legs 111, 137, 140, and 148). Proc. Ocean Drill. Progr. Sci. Res., 417-434.

Alt, J.C., Schwarzenbach, E.M., Fruh-Green, G.L., Shanks III, W.C., Bernasconi, S.M., Garrido, C.J., Crispini, L., Gaggero, L., Padron-Navarta, J.A., Marchesi, C., 2013. The role of serpentinites in cycling of carbon and sulfur: Seafloor serpentinization and subduction metamorphism. Lithos 178, 40-54.

Alt, J.C., Teagle, D.A.H., 2003. Hydrothermal alteration of upper oceanic crust formed at a fast spreading ridge: mineral, chemical, and isotopic evidence from ODP Site 801. Chem. Geol. 201, 191-211.

Alt, J.C., Teagle, D.A.H., Laverne, C., Vanko, D., Bach, W., Honnorez, J., Becker, K., Ayadi, M., and Pezard, P.A., 1996. Ridge flank alteration of upper ocean crust in the eastern Pacific: a synthesis of results for volcanic rocks of holes 504B and 896A. In Proceedings of the Ocean Drilling Program, Scientific Results , Vol. 148, eds. J.C. Alt, H. Kinoshita, L.B. Stokking, and P.J. Michael. College Station, TX: Ocean Drilling Program, pp. 434–452.

Angiboust, S., Agard, P., 2010. Initial water budget: The key to detaching large volumes of eclogitized oceanic crust along the subduction channel? Lithos 120, 453-474.

Angiboust, S., Agard, P., Jolivet, L., Beyssac, O., 2009. The Zermatt–Saas ophiolite: the largest (60 km wide) and deepest (c. 70–80 km) continuous slice of oceanic lithosphere detached from a subduction zone? Terra Nova, 21, 171–180.

Angiboust, S., Agard, P., Raimbourg, H., Yamato, P., Huet, B., 2011. Subduction interface processes recored by eclogite-facies shear zones (Monviso, W. Alps). Lithos 127, 222-238.

Angiboust, S., Langdon, R., Agard, P., Waters, D., Chopin, C., 2012. Eclogitization of the Monviso ophiolite (W. Alps) and implications on subduction dynamics. Jour. Metamorphic Petrol. 30, 37-61.

Angiboust, S., Pettke, T., de Hoog, J.C.M., Caron, B., Oncken, O., 2014. Channelized fluid flow and eclogite-facies metasomatism along the subduction shear zone. Jour. Petrol. 55, 883-916.

Artemyev, D.A., Zaykov, V.V., 2010. The types and genesis of ophicalcites in lower Devonian olistostromes at cobalt-bearing massive sulfide deposits in the West Magnitogorsk paleoisland arc (South Urals). Russ. Geol. Geophys. 51, 750–763.

Barbieri, M., Masi, U., Tolomeo, L., 1979. Stable isotope evidence for a marine origin of ophicalcites from the north-central Apennines (Italy). Mar. Geol. 30, 193–204. doi:10.1016/0025-3227 (79)90015-X.

Barnicoat, A.C., Cartwright, I., 1995. Focused fluid flow during subduction: Oxygen isotope data from high-pressure ophiolites of the western Alps. Earth Planet. Sci. Lett. 132, 53-61.

Barrett, T.J., Friedrichsen, H., 1989. Stable isotopic composition of atypical ophiolitic rocks from east Liguria, Italy. Chem. Geol. Isot. Geosci. Sect. 80(1), 71–84. doi: 10.1016/0168-9622(89)90049-3.

Bebout, G.E., 1991. Geometry and mechanisms of fluid flow at 15 to 45 kilometer depths in an early Cretaceous accretionary complex. Geophys. Res. Lett. 18, 923-926.

Bebout, G.E., 1995. The impact of subduction-zone metamorphism on mantle-ocean chemical cycling. Chem. Geol. 126, 191-218.

Bebout, G.E., 2007a. Metamorphic chemical geodynamics of subduction zones. Earth Planet. Sci. Lett. 260, 373-393.

Bebout, G.E., 2007b. Ch. 3.20. Trace element and isotopic fluxes/subducted slab, for Rudnick, R.L., ed., The Crust, Treatise on Geochemistry, Elsevier (eds. K. K. Turekian, H. D. Holland, and R. Rudnick), doi:10.1016/B978-008043751-4/00231-5.

Bebout, G.E., 2013. Chapter 9. Metasomatism in subduction zones of subducted oceanic slabs, mantle wedges, and the slab-mantle interface, in Harlov, D., and Austrheim, H., eds., Metasomatism and the Chemical Transformation of Rock, The Role of Fluids in Terrestrial and Extraterrestrial Processes, Springer-Verlag, pp. 289-349.

Bebout, G.E., 2014. 4.20. Chemical and isotopic cycling in subduction zones, in Rudnick, R. L., ed., The Crust, Treatise on Geochemistry (eds. H. D. Holland and K. K. Turekian, Second Edition), Elsevier-Pergamon, Oxford, pp. 703-747.

Bebout, G.E., Agard, P., Kobayashi, K., Moriguti, T., Nakamura, E., 2013. Devolatilization history, and related trace element mobility, in deeply subducted sedimentary rocks: SIMS evidence from Western Alps HP/UHP suites. Chem. Geol. 342, 1-20.

Bebout, G.E., Barton, M.D., 1993. Metasomatism during subduction: products and possible paths in the Catalina Schist, California. Chem. Geol. 108, 61-92.

Bebout, G.E., Fogel, M.L., 1992. Nitrogen-isotope compositions of metasedimentary rocks in the Catalina, California - Implications for metamorphic devolatilization history. Geochim. Cosmochim. Acta 56, 2839-2849.

Becker, H., Altherr, R., 1992. Evidence from ultra-high pressure marbles for recycling of sediments into the mantle. Nature 358, 745-748.

Beinlich, A., Klemd, R., John, T., and Gao, J., 2010, Trace-element mobilization during Ca-metasomatism along a major fluid conduit: Eclogitization of blueschist as a consequence of fluid–rock interaction. Geochim. Cosmochim. Acta 74, 1892-1922.

Berner, R.A., 1999. A new look at the long-term carbon cycle. GSA Today 9, 1-6.

Berner, R.A., Lasaga, A.C., Garrels, R.M., 1983. The carbonate-silicate geochemical cycle and its effect on atmospheric carbon dioxide over the past 100 million years. Amer. Jour. Sci. 283, 641-683.

Breeding, C.M., Ague, J.J., Bröcker, M., 2004. Fluid-metasedimentary interactions in subduction zone mélange: implications for the chemical composition of arc magmas. Geology 32, 1041-1044.

Brotzu, P., Ferrini, V., Masi, U., Morbidelli, L., Turi, B., 1973. Contributo alla conoscenza delle «Rocce Verdi» dell'Appennino centrale. Nota III. La composizione isotopica della calcite presente in alcuni affioramenti di oficalciti del F 129 (S. Fiora) e sue implicazioni petrologiche. Period. Mineral. 42, 591–619.

Busigny, V., Cartigny, P., Philippot, P., Ader, M., Javoy, M., 2003. Massive recycling of nitrogen and other fluid-mobile elements (K, Rb, Cs, H) in a cold slab environment: evidence from HP to UHP oceanic metasediments of the Schistes Lustres nappe (western Alps, Europe). Earth Planet. Sci. Lett. 215, 27-42.

Caciagli, N.C., Manning, C.E., 2003. The solubility of calcite in water at 6-16 kbar and 500-800 °C. Contrib. Mineral. Petrol. 146, 275-285

Cannat, M., Lagabrielle, Y., Bougault, H., Casey, J., De Coutures, N., Dmitriev, L., 1997. Ultramafic and gabbroic exposures at the Mid-Atlantic ridge: geological mapping in the 151N region. Tectonophys. 279, 197–213.

Cartwright, I., Barnicoat, A.C., 1999. Stable isotope geochemistry of Alpine ophiolites: a window to ocean-floor hydrothermal alteration and constraints on fluid-rock interaction during high-pressure metamorphism. Int. J. Earth Sci. 88, 219-235.

Cartwright, I. Barnicoat, A.C., 2003. Geochemical and stable isotope resetting in shear zones from Taschalp: constraints on fluid flow during exhumation in the Western Alps. Jour. Metamorphic Geol. 21, 143-161.

Castelli, D., Rolfo, F., Groppo, C., Compagnoni, R., 2007. Impure marbles from the UHP Brossasco-Isasca Unit (Dora-Maira Massif, western Alps): evidence for Alpine equilibration in the diamond stability field and evaluation of the X(CO_2) fluid evolution. Jour. Metamorphic Geol. 25, 587-603.

Clerc, C., Boulvais, P., Lagabrielle, Y., de Saint Blanquat, M., 2014. Ophicalcites from the northern Pyrenean belt: a field, petrographic and stable isotope study. Int. J. Earth Sci. 103(1), 141-163.

Coggon, R.M., Teagle, D.A.H., Smith-Duque, C.E., Alt, J.C., Cooper, M.J., 2010. Reconstructing past seawater Mg/Ca and Sr/Ca from mid-ocean ridge flank calcium carbonate veins. Science 327, 1114-1117.

Connolly, J.A.D., 2005. Computation of phase equilibria by linear programming: a tool for geodynamic modeling and its application to subduction zone decarbonation. Earth Planet. Sci. Lett. 236, 524-541.

Cook-Kollars, J., Bebout, G.E., Collins, N.C., Angiboust, S., Agard, P., 2014. Subduction zone metamorphic pathway for deep carbon cycling: Evidence from HP/UHP metasedimentary rocks, Italian Alps. Chem. Geol., doi: 10.1016/j.chemgeo.2014.07.013.

Dasgupta, R., 2013. Ingassing, storage, and outgassing of terrestrial carbon through geologic time. Mineral. Soc. Amer. Rev. Mineral. Geochem. 75, 183-229.

Dasgupta, R., Hirschmann, M.M., 2010. The deep carbon cycle and melting in Earth's interior. Earth Planet. Sci. Lett. 298, 1-13.

de Leeuw, G.A.M., Hilton, D.R., Fischer, T.P., Walker, J.A., 2007. The He-CO_2 isotope and relative abundance characteristics of geothermal fluids in El Salvador and Honduras: New constraints on volatile mass balance of the Central American Volcanic Arc. Earth Planet. Sci. Lett. 258, 132-146.

Demeny, A., Vennemann, T., Koller, F., 2007. Stable isotope compositions of the Penninic ophiolites of the Köszeg-Rechnitz series. Central. Eur. Geol. 50(1), 29–46, doi:10.1556/CEuGeol.50.2007.1.3.

Desmons, J., Aprahamian, J., Compagnoni, R., Cortesogno, L., Frey, M., 1999a. Alpine metamorphism of the Western Alps: I. Middle to high T/P metamorphism. Schweiz. Mineral. Petrogr. Mitt. 79, 89–110.

Desmons, J., Aprahamian, J., Compagnoni, R., Cortesogno, L., Frey, M., 1999b. Alpine metamorphism of the Western Alps: II. High P/T and related pre-greenschist metamorphism. Schweiz. Mineral. Petrogr. Mitt. 79, 111-134.

Ernst, W.G., Dal Piaz, G.V., 1978. Mineral parageneses of eclogitic rocks and related mafic schists of the Piemonte ophiolite nappe, Breuil-St. Jacques area, Italian Western Alps. Amer. Mineral. 63, 621-640.

Evans, C.A., Baltuck, M., 1988. Low-temperature alteration of peridotite, hole 637A. In: Boillot G, Winterer EL et al (ed.) Proc. Ocean Drill. Progr. Sci. Res., 103, 235–239, http://www.odp.tamu.edu/publications/103_SR/103TOC.HTML.

Facq, S., Daniel, I., Montagnac, G., Cardon, H., Sverjensky, D.A., 2014. *In situ* Raman study and thermodynamic model of aqueous carbonate speciation in equilibrium with aragonite under subduction zone conditions. Geochim. Cosmochim. Acta 132, 375-390.

Frezzotti, M.L., Huizenga, J.M., Compagnoni, R., Selverstone, J., 2014. Diamond formation by carbon saturation in C-O-H fluids during cold subduction of oceanic lithosphere. Geochim. Cosmochim. Acta, http://dx.doi.org/10.1016/j.gca.2013.12.022.

Frezzotti, M.L., Selverstone, J., Sharp, Z.D., Compagnoni, R., 2011. Carbonate dissolution during subduction revealed by diamond-bearing rocks from the Alps. Nature Geosci. 4, 703-706.

Furnes, H., Muehlenbachs, K., Torsvik, T., Thorseth, I.H., Tumyr, O., 2001. Microbial fractionation of carbon isotopes in altered basaltic glass from the Atlantic Ocean, Lau Basin and Costa Rica Rift. Chem. Geol. 173, 313-330.

Fusseis, F., Regenauer-Lieb, K., Liu, J., Hough, R.M., De Carlo, F., 2009. Creep cavitation can establish a dynamic granular fluid pump in ductile shear zones. Nature 459, 974-977.

Galvez, M.E., Beyssac, O., Martinez, I., Benzerara, K., Chaduteau, C., Malvoisin, B., Malavielle, J., 2013. Graphite formation by carbonate reduction during subduction. Nature Geosci., DOI: 10.1038/NGEO1827.

Gao, J., John, T., Klemd, R., Xiong X., 2007. Mobilization of Ti–Nb–Ta during subduction: evidence from rutile-bearing dehydration segregations and veins hosted in eclogite, Tianshan, NW China. Geochim. Cosmochim. Acta 71, 4974–4996.

Gao, J., Klemd, R., 2003. Formation of HP-LT rocks and their tectonic implications in the western Tianshan Orogen, NW China; geochemical and age constraints. Lithos 66, 1-22.

Gasparik, T., 1989. Experimental study of subsolidus phase relations and mixing properties of pyroxene and plagioclase in the system Na_2O-CaO-Al_2O_3-SiO_2, Contrib. Mineral. Petrol. 89 346-357.

Gebauer, D., Schertl, H.-P., Brix, M., Schreyer, W., 1997. 35 Ma old ultrahigh-pressure metamorphism and evidence for very rapid exhumation in the Dora Maira massif, Western Alps. Lithos 41, 5–24.

Gerya, T.V., Stockhert, B., Perchuk, A.L., 2002. Exhumation of high-pressure metamorphic rocks in a subduction channel: A numerical simulation. Tectonics 21, doi:10.1029/2002TC001406, 2002.

Gillis, K.M., Coogan, L.A., 2011. Secular variation in carbon uptake into the oceanic crust. Earth Planet. Sci. Lett. 302, 385-392.

Gorman, P.J., Kerrick, D.M., Connolly, J.A.D., 2006. Modeling open system metamorphic decarbonation of subducting slabs. Geochem. Geophys. Geosyst. 7, Q04007, doi:10.1029/2005GC001125.

Groppo, C., Beltrando, M., Compagnoni, R., 2009. The P-T path of the ultra-high pressure Lago di Cignana and adjoining high-pressure meta-ophiolitic units: insights into the evolution of the subducting Tethyan slab. Jour. Metamorphic Geol. 27, 207-231.

Halldorsson, S.A., Hilton, D.R., Troll, V.R., Fischer, T.P., 2013. Resolving volatile sources along the western Sunda arc, Indonesia. Chem. Geol. 339, 263-282.

Herms, P., John, T., Bakker, R.J., Schenk, V., 2012. Evidence for channelized external fluid flow and element transfer in subducting slabs (Raspas Complex, Ecuador). Chem. Geol. 310-311, 79-96.

Hilton, D.R., Fischer, T.P., Marty, B., 2002. Noble gases and volatile recycling at subduction zones. Rev. Mineral. Geochem. 47, 319.

Holland, T., Powell, R., 1991. A Compensated-Redlich-Kwong (CORK) equation for volumes and fugacities of CO_2 and H_2O in the range 1 bar to 50 kbar and 100–1600 ˚C. Contrib. Mineral. Petrol. 109, 265-273.

Holland, T.J.B., Powell, R., 1998. An internally consistent thermodynamic data set for phases of petrological interest. Jour. Metamorphic Geol. 16, 309-343.

House, B.M., Bebout, G.E., Hilton, D.R., Rodriguez, B., Plank, T., 2014. Constraining sources of subducted and recycled carbon along the Sunda Arc (abstract), Amer. Geophys. Un. Ann. Meeting, San Francisco, December, 2014.

Jarrard, R.D., 2003. Subduction fluxes of water, carbon dioxide, chlorine, and potassium. Geochem. Geophys. Geosyst. 5; doi:10.1029/2002GC000392.

Javoy, M.,1998. The birth of the Earth's atmosphere: the behaviour and fate of its major elements. Chem. Geol. 147, 11-25.

Jedrysek, M.O., Weber-Weller, A., Szynkiewicz, A., Mierzejewski, M., 2000, Evolution of Sleza and Nowa Ruda Ophiolites: Oceanic and Continental Stages Recorded in Stable Isotope Composition of Oxides, Carbonates and Sulphides. GeoLines (Praha) 10.

Joesten, R., 1977. Evolution of mineral assemblage zoning in diffusion metasomatism. Geochim. Cosmochim. Acta 41, 649-670.

John, T., Gussone, N., Podladchikov, Y.Y., Bebout, G.E., Dohmen, R., Halama, R., Klemd, R., Magna, T., Seitz, H.M., 2012. Volcanic arcs fed by rapid pulsed fluid flow through subducting slabs, Nature Geosci. 5, 489-492.

John, T., Klemd, R., Gao, J., Garbe-Schonberg, C.D., 2008, Trace-element mobilization in slabs due to non steady-state fluid-rock interaction: constraints from an eclogite-facies transport vein in blueschist (Tianshan, China). Lithos 103, 1-24.

John, T., Schenk, V., 2003. Partial eclogitisation of gabbroic rocks in a late Precambrian subduction zone (Zambia): prograde metamorphism triggered by fluid infiltration. Contrib. Mineral. Petrol. 146, 174-191.

Jolivet, L., Faccena, C., Goffe, B., Burov, E., Agard, P., 2003. Subduction tectonics and exhumation of high-pressure metamorphic rocks in the Mediterranean orogens. Amer. Jour. Sci. 303, 353-409.

Kato, T., Enami, M. Zhai, M., 1997. Ultra-high-pressure (UHP) marble and eclogite in the Su-Lu UHP terrane, eastern China. Jour. Metamorphic Geol. 15, 169–182.

Kerrick, D.M., 2001. Present and past nonanthropogenic CO_2 degassing from the solid Earth. Rev. Geophys. 39, 565-585.

Kerrick, D.M., Connolly, J.A.D., 1998. Subduction of ophicarbonates and recycling of CO_2 and H_2O. Geology 26, 375-378.

Kerrick, D.M., Connolly, J.A.D., 2001a. Metamorphic devolatilization of subducted marine sediments and the transport of volatiles into the Earth's mantle. Nature 411, 293-296.

Kerrick, D.M., Connolly, J.A.D., 2001b. Metamorphic devolatilization of subducted oceanic metabasalts: implications for seismicity, arc magmatism and volatile recycling. Earth Planet. Sci. Lett. 189, 19-29.

King, R.L., Bebout, G.E., Grove, M., Moriguti, T., Nakamura, E., 2007. Boron and lead isotope signatures of subduction-zone melange formation: Hybridization and fractionation along the slab-mantle interface beneath volcanic arcs. Chem. Geol. 239, 305-322.

King, R.L., Bebout, G.E., Kobayashi, K., Nakamura, E., van der Klauw, S.N.G.C., 2004. Ultrahigh-pressure metabasaltic garnets as probes into deep subduction zone chemical cycling. Geochem. Geophys. Geosyst., Q12J14, doi:10.1029/2004GC000746.

King, R.L., Bebout, G.E., Moriguti, T., Nakamura, E., 2006. Elemental mixing systematics and Sr-Nd isotope geochemistry of mélange formation: Obstacles to identification of fluid sources to arc volcanics. Earth Planet. Sci. Lett. 246, 288-304.

Klemd, R., Schroter, F.C., Will, T.M. Gao, J., 2002. P-T evolution of glaucophane-omphacite bearing HP-LT rocks in the western Tianshan Orogen, NW China; new evidence for "Alpine-type" tectonics. Jour. Metamorphic Geol. 20, 239-254.

Klemd, R., Bröcker, M., Hacker, B.R., Gao, J., Gans, P., Wemmer, K., 2005. New age constraints on the metamorphic evolution of the high-pressure/low-temperature belt in the western Tianshan Mountains, NW China. Jour. Geol. 113, 157-168.

Klemd, R., John, T., Scherer, E.E., Rondenay, S., Gao, J., 2011. Changes in dip of subducted slabs at depth: Petrological and geochronological evidence from HP-UHP rocks (Tianshan, NW-China). Earth Planet. Sci. Lett., 310, 9-20.

Konrad-Schmolke, M., Halama, R., 2014. Combined thermodynamic-geochemical modeling in metamorphic geology: Boron as tracer of fluid-rock interaction. Lithos 208-209, 393-414.

Lagabrielle, Y., Cannat, M., 1990. Alpine Jurassic ophiolites resemble the modern central Atlantic basement. Geology 18, 319-322.

Lavoie, D., Cousineau, P.A., 1995. Ordovician ophicalcites of southern Quebec Appalachians: a proposed early seafloor tectonosedimentary and hydrothermal origin. Jour. Sediment. Res. 65(2a), 337–347.

Lazar, C., Zhang, C., Manning, C.E., Mysen, B.O., 2014. Redox effects on calcite-portlandite-fluid equilibria at forearc conditions: Carbon mobility, methanogenesis, and reduction melting of calcite. Amer. Mineral. 99, 1604-1615.

Leoni, L., Marroni, M., Sartori, F., Tamponi, M., 1996. Metamorphic grade in metapelites of the internal liguride units (Northern Apennines, Italy). Eur. J. Min. 8(1), 35-50.

Li, L., Bebout, G.E., 2005. Carbon and nitrogen geochemistry of sediments in the Central American convergent margin: Insights regarding subduction input fluxes, diagenesis, and paleoproductivity. Jour. Geophys. Res. 110, B11202.

Lu, Z., Zhang, L., Chen, Z., 2014. Jadeite- and dolomite-bearing coesite eclogite from western Tianshan, NW China. Eur. J. Mineral. 26, 245-256.

Manning, C.E., 2014. A piece of the deep carbon puzzle (News & Views). Nature Geosci., April 20, 2014.

Manning, C.E., Shock, E.L., Sverjensky, D.A., 2013. The chemistry of carbon in aqueous fluids at crustal and upper-mantle conditions: Experimental and theoretical constraints. Mineral. Soc. Amer. Rev. Mineral. Geochem. 75, 109-148.

Marin-Ceron, M.I., Moriguti, T., Makishima, A., Nakamura, E., 2010. Slab decarbonation and CO_2 recycling in the Southwestern Colombian volcanic arc. Geochim. Cosmochim. Acta 74, 1104-1121.

Martin, S., Rebay, G., Kienast, J.-R., Mevel, C., 2008. An eclogitised oceanic paleohydrothermal field from the St. Marcel Valley (Italian Western Alps). Ofioliti 33, 49-63.

Martin, S., Tartarotti, P., 1989. Polyphase HP Metamorphism in the ophiolitic gaucophanites of the Lower St. Marcel Valley (Aosta, Italy). Ofioliti 14. 135–156.

Marty, B., Tolstikhin, I.N., 1998. CO_2 fluxes from mid-ocean ridges, arcs and plumes. Chem. Geol. 145, 233-248.

Michard, A., Avigad, D., Goffe, B., Chopin, C., 2004. The high-pressure metamorphic front of the south Western Alps (Ubaye-Maira transect, France, Italy). Schweiz. Mineral. Petrogr. Mitt. 84, 215-235.

Miller, J.A., Cartwright, I., 2000. Distinguishing between seafloor alteration and fluid flow during subduction using stable isotope geochemistry: examples from Tethyan ophiolites in the Western Alps. Jour. Metamorphic Geol. 8, 467-482.

Miller, J.A., Cartwright, I., Buick, I.S. Barnicoat, A.C., 2001. An O-isotope profile through the HP-LT Corsican ophiolite, France and its implications for fluid flow during subduction. Chem. Geol. 178, 43-69.

Miller, D.P., Marschall, H.R., Schumacher, J.C., 2009. Metasomatic formation and petrology of blueschist-facies hybrid rocks from Syros (Greece): Implications for reactions at the slab-mantle interface, Lithos 107, 53-67.

Milliken, K.L., Morgan, J.K., 1996. Chemical evidence for near-seafloor precipitation of calcite in serpentinites (site 897) and Serpentinite Breccias (Site 899), Iberia Abyssal Plain. In: Whitmarsh RB, Sawyer DS, Klaus A, Masson DG (eds) Proceedings of the ocean drilling program, 149 scientific results, vol. 149, Ocean Drilling Program, pp. 553–558, http://www-odp.tamu.edu/publications/149_SR/149TOC.HTML

Molina, J. F., and Poli, S., 2000. Carbonate stability and fluid composition in subducted oceanic crust: an experimental study on H_2O-CO_2-bearing basalts. Earth Planet. Sci. Lett. 176, 295-310.

Nadeau, S., Philippot, P. Pineau, F., 1993. Fluid inclusion and mineral isotopic compositions (H-C-O) in eclogitic rocks as tracers of local fluid migration during high-pressure metamorphism. Earth Planet. Sci. Lett. 114, 431-448.

Parrish, R.R., Gough, S.J., Searle, M.P., Waters, D.J., 2006. Plate velocity exhumation of ultra-high pressure eclogites in the Pakistan Himalaya. Geology 34, 989–992.

Pelletier, L., Muntener, O., Kalt, A., Vennemann, T.W., Belgya, T., 2008. Emplacement of ultramafic rocks into the continental crust monitored by light and other trace elements: An example from the Geisspfad body (Swiss-Italian Alps). Chem. Geol. 255, 143-159.

Penniston-Dorland, S.C., Kohn, M.J., Manning, C.E., 2014. Exhumed blueschists and eclogites: hotter than the average model. Abstract V24C-06, Amer. Geophys. Union Fall Meeting.

Penniston-Dorland, S.C., Kohn, M.J., Manning, C.E., in press. The global range of subduction zone thermal structures from exhumed blueschists and eclogites: Rocks are hotter than models. Earth Planet. Sci. Lett.

Philippot, P., 1993. Fluid-melt-rock interaction in mafic eclogites and coesite-bearing metasediments: constraints on volatile.recycling during subduction. In: J.L.R. Touret and A.B. Thompson (Guest-Editors), Fluid-Rock Interaction in the Deeper Continental Litbosphl:re. Chem. Geol. 108, 93-112 (special issue).

Philippot, P., Selverstone, J., 1991. Trace element-rich brines in eclogitic veins: implications for fluid composition and transport during subduction. Contrib. Mineral. Petrol. 106, 417–430.

Plank T., 2014, 4.19. The chemical composition of subducting sediments, in Rudnick, R.L. (Ed.), The Crust, Treat. Geochem., 2nd edition, v. 4, Elsevier.

Plank, T., Langmuir, C.H., 1998. The chemical composition of subducting sediment and its consequences for the crust and mantle. Chem. Geol. 145, 325-394.

Plas, A., 1997. Petrologic and stable isotope constraints on fluid-rock interaction, serpentinization and alteration of oceanic ultramafic rocks. PhD Thesis, Swiss Federal Institute of Technology.

Platt, J.P., 1986. Dynamics of orogenic wedges and the uplift of high-pressure metamorphic rocks. Geol. Soc. Amer. Bull. 97, 1037-1053.

Poli, S., Franzolin, E., Fumagalli, P., Crottini, A., 2009. The transport of carbon and hydrogen in subducted oceanic crust: An experimental study to 5 GPa. Earth Planet. Sci. Lett. 278, 350-360.

Proyer, A., 2003. Metamorphism of pelites in NKFMASH – a new petrogenetic grid with implications for the preservation of high-pressure mineral assemblages during exhumation. Jour. Metamorphic Geol. 21, 493-509.

Proyer, A., Rolfo, F., Castelli, D., Compagnoni, R., 2014. Diffusion-controlled metamorphic reaction textures in an ultrahigh-pressure impure calcite marble from Dabie Shan, China. Eur. J. Mineral. 26, 25-40.

Ranero, C.R., Villasenor, A., Phipps Morgan, J., Weinrebe, W., 2005. Relationship between bend-faulting at trenches and intermediate-depth seismicity. Geochem. Geophys. Geosyst. 6, Q12002, doi:10.1029/2005GC000997.

Reinecke, T., 1998. Prograde high- to ultrahigh-pressure metamorphism and exhumation of oceanic sediments at Lago di Cignana, Zermatt-Saas Zone, western Alps. Lithos 42, 147-189.

Rubatto, D., Gebauer, D., Fanning, M., 1998. Jurassic formation and Eocene subduction of the Zermatt-Saas-Fee ophiolites: implications for the geodynamic evolution of the Central and Western Alps. Contrib. Mineral. Petrol. 132, 269-287.

Rubatto, D., Hermann, J., 2001. Exhumation as fast as subduction? Geology 29, 3–6.

Rubatto, D., Hermann, J., 2003. Zircon formation during fluid circulation in eclogites (Monviso, Western Alps): implications for Zr and Hf budget in subduction zones. Geochim. Cosmochim. Acta 67, 2173-2187.

Sadofsky, S.J., Bebout, G.E., 2003. Record of forearc devolatilization in low-T, high-P/T metasedimentary suites: significance for models of convergent margin chemical cycling, Geochem. Geophy. Geosyst. 4, 9003, doi:10.1029/2002GC000412.

Sano, Y., Williams, S.N., 1996. Fluxes of mantle and subducted carbon along convergent margins. Geophys. Res. Lett. 23, 2749-2752.

Sano, Y., Takahata, N., Nishio, Y., Fischer, T.P., Williams, S.N., 2001. Volcanic flux of nitrogen from the Earth. Chem. Geol. 171, 263-271.

Scambelluri, M., Malaspina, N., Hermann, J., 2007. Subduction fluids and their interaction with the mantle wedge: a perspective from the study of high-pressure ultramafic rocks. Periodico di Mineralogia 76, 253-265.

Scambelluri, M., Muntener, O., Ottolini, L., Pettke, T., Vannucci, R., 2004. The fate of B, Cl, and Li in the subducted oceanic mantle and in the antigorite breakdown fluids. Earth Planet. Sci. Lett. 222, 217-234.

Scambelluri, M., Philippot, P., 2001. Deep fluids in subduction zones. Lithos 55, 213-227.

Schmidt, M.W., Poli, S., 2014. 4.19. Devolatilization during subduction, in Rudnick, R. L., ed., The Crust, Treatise on Geochemistry (eds. H. D. Holland and K. K. Turekian, Second Edition), Elsevier-Pergamon, Oxford, pp. 669-701.

Scholl, D.W., von Huene, R., 2010. Subduction zone recycling processes and the rock record of crustal suture zones. Can. Jour. Earth Sci. 47, 633-654.

Schwarzenbach, E.M., Fruh-Green, G.L., Bernasconi, S.M., Alt, J.C., Plas, A., 2013. Serpentinization and carbon sequestration: A study of two ancient peridotite-hosted hydrothermal systems. Chem. Geol. 351, 115-133.

Shaw, A.M., Hilton, D.R., Fischer, T.P., Walker, J.A., Alvarado, G.E., 2003. Contrasting He–C relationships in Nicaragua and Costa Rica: insights into C cycling through subduction zones. Earth Planet. Sci. Lett. 214, 499–513.

Sheppard, S.M.F., Schwarcz, H.P., 1970. Fractionation of carbon and oxygen isotopes and magnesium between coexisting metamorphic calcite and dolomite. Contrib. Mineral. Petrol. 26, 161-198.

Skelton, A.D., Valley, J.W., 2000. The relative timing of serpentinisation and mantle exhumation at the ocean-continent transition, Iberia: constraints from oxygen isotopes. Earth. Planet. Sci. Lett. 178, 327–338.

Spandler, C., Hermann, J., 2006. High-pressure veins in eclogite from New Caledonia and their significance for fluid migration in subduction zones. Lithos 89, 135-153.

Spandler, C., Pettke, T., Rubatto, D., 2011. Internal and external fluid sources for eclogite-facies veins in the Monviso meta-ophiolite, Western Alps: Implications for fluid flow in subduction zones. Jour. Petrol. 52, 1207-1236.

Staudigel, H., Hart, S.R., Schmincke, H.U., Smith, B.M., 1989. Cretaceous ocean crust at DSDP Sites 417 and 418: Carbon uptake from weathering versus loss by magmatic outgassing. Geochim. Cosmochim. Acta 53, 3091-3094.

Staudigel, H., Plank, T., White, B., Schmincke, H.U., 1996. Geochemical fluxes during seafloor alteration of the basaltic upper oceanic crust: DSDP Sites 417 and 418. in Bebout, G.E., Scholl, D.W., Kirby, S.H., Platt, J.P., eds., Subduction Top to Bottom, Amer. Geophys. Un. Geophys. Monogr. 96, 19-38.

Syracuse, E.M., Abers, G.A., 2006. Global compilation of variations in slab depth beneath arc volcanoes and implications. Geochem. Geophys. Geosyst. Q05017, doi:10.1029/2005GC001045.

Syracuse, E.M., van Keken, P.E., Abers, G.A., 2010. The global range of subduction zone thermal models. Phys. Earth Planet. Int. 183, 73-90.

Thompson, A.B., 1975. Calc-silicate diffusion zones between marble and pelitic schist. Jour. Petrol. 16, 314-346.

Tricart, P., Lemoine, M., 1986. From faulted blocks to megamullions and megaboudins: Tethyan heritage in the structure of the Western Alps. Tectonics 5, 95-118.

Tricart, P., Lemoine, M., 1991. The Queyras ophiolite west of Monte Viso (Western Alps): indicator of a peculiar ocean floor in the Mesozoic Tethys. Jour. Geodynam. 13, 163-181.

Tsuno, K., Dasgupta, R., 2011. Melting phase relation of nominally anhydrous, carbonated pelitic-eclogite at 2.5-3.0 GPa and deep cycling of sedimentary carbon. Contrib. Mineral. Petrol. 161, 743-763.

Tsuno, K., Dasgupta, R., Danielson, L., Righter, K., 2012. Flux of carbonate melt from deeply subducted pelitic sediments: Geophysical and geochemical implications for the source of Central American volcanic arc. Geophys. Res. Lett. 39, doi:10.1029/2012GL052606.

Valley, J.W., 1986. Stable isotope geochemistry of metamorphic rocks. Rev. Mineral. Geochem. 16, 445-489.

Vallis, F., Scambelluri, M., 1996. Redistribution of high-pressure fluids during retrograde metamorphism of eclogite-facies rocks (Voltri Massif, Italian Western Alps). Lithos 39, 81-92.

van der Meer, D.G., Zeebe, R.E., van Hinsbergen, D.J.J., Sluijs, A., Spakman, W., Torsvik, T.H., 2014. Plate tectonic controls on atmospheric CO_2 levels since the Triassic. Proc. National Acad. Sci. 111, 4380-4385.

van der Klauw, S.N.G.C., 1998. Exhumation of ultrahigh-pressure metamorphic oceanic crust from Lago di Cignana, Piemontese zone, western Alps: the structural record in metabasites. PhD Thesis, Ruhr-Universität Bochum.

van der Klauw, S.N.G.C., Reinecke, T., Stockhert, B., 1997. Exhumation of ultrahigh-pressure metamorphic oceanic crust from Lago di Cignana, Piemontese zone, western Alps: the structural record in metabasites. Lithos 41, 79-102.

van der Straaten, F., Schenk, V., John, T., Gao, J., 2008. Blueschist-facies rehydration of eclogites (Tian Shan, NW-China): Implications for fluid-rock interaction in the subducted channel. Chem. Geol. 255, 195-219.

van der Straaten, F., Halama, R., John, T., Schenk, V., Hauff, F., Andersen, N., 2012. Tracing the effects of high-pressure metasomatic fluids and seawater alteration in blueschist-facies overprinted eclogites: Implications for subduction channel processes. Chem. Geol. 292, 69-87.

van Keken, P.E., Hacker, B.R., Syracuse, E.M., Abers, G.A., 2011. Subduction factory: 4. Depth-dependent flux of H_2O from subducting slabs worldwide. Jour. Geophys. Res. 116, B01401, doi:10.1029/2010JB007922.

Vignaroli, G., Rossetti, F., Bouybaouene, M., Massonne J., Theye, T., Faccenna, C., Funiciello, R., 2005, A counter-clockwise P–T path for the Voltri Massif eclogites (Ligurian Alps, Italy). Jour. Metamorphic Geol. 23, 533-555.

Wei, C., Powell, R., 2003. Phase relations in high-pressure metapelites in the system KFMASH (K_2O-FeO-MgO-Al_2O_3-SiO_2-H_2O) with application to natural rocks. Contrib. Mineral. Petrol. 145, 301-315.

Wei, C., Powell, R., Zhang, L., 2003. Eclogites from the south Tianshan, NW China: petrological characteristic and calculated mineral equilibria in the Na_2O-CaO-FeO $MgOAl_2O_3$-SiO_2-H_2O system. Jour. Metamorphic Geol. 21, 163-179.

Weissert, H., Bernoulli, D., 1984. Oxygen isotope composition of calcite in Alpine ophicarbonates: a hydrothermal or Alpine metamorphic signal? Eclogae. Geol. Helv. 77(1), 29–43.

Whitney, D.L., Evans, B.W., 2010. Abbreviations for names of rock-forming minerals. Amer. Mineral. 95(1), 185.

Widmer, T., Thompson, A.B., 2001. Local origin of high pressure vein material in eclogite facies rocks of the Zermatt-Saas Zone, Switzerland. Amer. Jour. Sci. 301, 627-656.

Zack, T., John, T., 2007. An evaluation of reactive fluid flow and trace element mobility in subducting slabs. Chem. Geol. 239, 199-216.

Zhang, Y., Zindler, A., 1993. Distribution and evolution of carbon and nitrogen in Earth. Earth Planet. Sci. Lett. 117(3), 331-345.

Zheng, Y.-F., 1993. Calculation of oxygen isotope fractionation in anhydrous silicate minerals. Geochim. Cosmochim. Acta 57, 1079-1091.

Zheng, Y.-F., 2012. Metamorphic chemical geodynamics in continental subduction zones. Chem. Geol. 328, 5-48, doi:10.1016/j.chemgeo.2012.02.005.

Zheng, Y.-F., Fu, B., Gong, B., Li, L., 2003. Stable isotope geochemistry of ultrahigh pressure metamorphic rocks from the Dabie-Sulu orogen in China: implications for geodynamics and fluid regime. Ear.-Sci. Rev. 62, 105-161.

Zimmer, M.M., Fischer, T.P., Hilton, D.R., Alvarado, G.E., Sharp, Z.D., Walker, J.A., 2004. Nitrogen systematics and gas fluxes of subduction zones: Insights from Costa Rica arc volatiles. Geochem. Geophy. Geosyst. 5, Q05J11, doi:10.1029/2003GC000651.

Figure Captions

Figure 1. (**A**) Generalized geologic map for the Western Alps detailing sample locations. See **Supplementary Table 1** for coordinates of sampling locations. (**B**) Pressure-temperature diagram showing peak *P-T* for the field localities and the *P-T* gradient defined by these units. *P-T* estimates for these locations are from Leoni et al. (1996), Michard et al. (2004), Angiboust et al. (2012), Vignaroli et al. (2005), Angiboust and Agard (2010), Groppo et al. (2009), and Frezzotti et al. (2011, 2014). Units for Monviso are denoted with LS for the Lago Superiore Unit and MV for the Monviso Unit.

Figure 2: Field photographs of pillow basalts with representative textures, all but (**C**) with a 35mm camera lens for scale. (**A**) Undeformeed prenhite-pumpellyite facies pillow basalts

from the Bracco Unit. (**B**) Eclogite facies pillow basalt from the Lago Superiore Unit at Monviso. (**C**) Deformed meta-pillow basalts at the Lago di Cignana locality (horizontal dimension ~1m). (**D**) Breccia containing clasts of metagabbro in a largely calcite matrix at the Bracco Unit exposure.

Figure 3: $\delta^{13}C$ and $\delta^{18}O$ for all of carbonate sampled from all textural settings within the metabasalts (data in **Supplementary Table 2**). The lower unfilled box on the right side of the plot illustrates the range of values for finely disseminated calcite in seafloor-altered basalts (from Furnes et al., 2001). The upper unfilled box shows the $\delta^{18}O$ range possible for carbonate veins in variably seafloor-altered basalts (from Alt and Teagle, 2003; Coggon et al., 2010; J. Alt and R. Coggon, personal communication, 2014). Also included are data for veins and breccia fillings in metabasalt from Catalina Schist from Bebout (1995). The curved line labeled "Rayleigh Trend" is the trend in $\delta^{13}C$ and $\delta^{18}O$ for closed-system decarbonation approximating a Rayleigh process (i.e., generation and loss of fluid without addition of fluid from external sources). The exact curve length (i.e., decrease in $\delta^{13}C$ possible, related to the fraction of C remaining in the Rayleigh calculation) and the trajectory taken depend on the initial modal abundances of the carbonate and silicate phases and the reactions that take place (the latter producing change in mineral modes). Whole-rock $\delta^{18}O$ values for seafloor-altered oceanic crust are as high as +20‰ but most are in the range of +5 to +10‰ (Alt, 2004). The arrow labeled, "Exchange with H_2O-rich Fluid," indicates the $\delta^{18}O$ shifts that carbonate in metabasalts would experience as influenced by exchange with H_2O-rich fluid containing little or no C (depending on temperature and the $\delta^{18}O$ of the fluids).

Figure 4: Carbon and O isotope plots for select localities divided by textural occurrence of carbonates. (**A**) Bracco and Mt. Fignona Units; (**B**) Monviso (Monviso Unit and Lago Supierore Unit); (**C**) Ubaye Unit, France, and (**D**) Zermatt-Saas and Lago di Cignana.

Figure 5: Isotopic compositions of the ophicarbonates (modified from Clerc et al., 2014; data in **Supplementary Table 2**). Shaded grey areas and lightly shaded grey symbols represent values from the literature for ophicalcites from the low-temperature Iberian margin and Galicia Bank (Evans and Baltuck, 1988; Milliken and Morgan, 1996; Plas, 1997; Skelton and Valley, 2000), the Alps, Apennines, and Pyrenees (Brotzu et al., 1973; Barbieri et al., 1979; Weissert and Bernoulli, 1984; Barrett and Friedrichsen, 1989; Demeny et al., 2007; Clerc et al., 2014), and from other high-temperature hydrothermal ophicalcites (Lavoie and Cousineau, 1995; Artemyev and Zaykov, 2010; Jedrysek et al., 2000).

Figure 6: Pseudosections calculated with Perple_X for different basalt compositions with *P-T* paths from four modern subduction zones (dashed white lines) from van Keken et al. (2011). T = Tonga, NV = N. Vanuatu, N = Nankai, and C= Cascadia. Basaltic compositions are from Staudigel et al. (1989), Alt et al. (1996), Staudigel et al. (1996), and King et al. (2004), and are provided in **Supplementary Table 4**. Mineral abbreviations are from Whitney and Evans (2010) with the exception of the combined carbonate phases (Carb). Note the very different starting CO_2 concentrations in these compositions. A recent comparison of peak-pressure *P-T* conditions for HP/UHP suites with recently published thermal models, by Penniston-Dorland et al. (2014, in press), indicates that the *P-T* paths calculated by Gerya et al. (2002) for forearcs could be more compatible with the field metamorphic record than those of Syracuse et al. (2010). However, the models of both Gerya et al. (2002) and Syracuse et al. (2010) compare reasonably well with the array of peak *P-T* for the W. Alps forearc units investigated in this study and by Cook-Kollars et al. (2014). The two thermal modeling

studies similarly indicate top-slab temperatures >600˚C at depths of 80-120 km (see the discussion in **Section 5.3**).

Figure 7: Mineral modal abundances calculated with Perple_X for four modern day subduction zones using the average composition of ODP 417/418 (see the pseudosection for this composition in **Fig. 6C**). **A** = Tonga; **B** = N. Vanuatu; **C** = Nankai; **D** = Cascadia. In these figures, the x axis indicates pressure increase to the right (and corresponding temperature increase) along the *P-T* paths for these margins shown in **Figs. 6, 8a, and 10**.

Figure 8. (**A**) Volatiles isopleth diagram of a composition from ODP Site 417/418 (Staudigel et al., 1996) containing a relatively high H_2O content. Dashed grey lines represent H_2O content and solid black lines represent the CO_2 content. Solid grey lines display *P-T* paths for four modern day subduction zones (Syracuse et al, 2010; van Keken et al., 2011) and are labeled the same as **Figs. 6C and 7**. Blue boxes represent the *P-T* estimates of the sites sampled in this study. (**B**) Closed-system devolatilization of the average composition from ODP 417/418 (Staudigel et al., 1996) across three modern day subduction zones (Tonga [cool], N. Vanuatu [intermediate], and Cascadia [warm]; see **A**). These *P-T* paths were taken from Syracuse et al. (2010) and van Keken et al. (2011; P. van Keken, personal communication, 2013). Light grey-shaded area represents metabasalts investigated in this study. The dark grey-shaded area represents the global average of modern day sub-arc depths.

Figure 9: T-X_{CO_2} diagrams from the average basaltic composition of ODP 417/418 (composition from Staudigel et al., 1996; see **Supplementary Table 4**). **Panel A** shows the compositions at 15 kbar and **Panel B** shows compositions at 25 kbar. **Panels 1-2** detail the modal abundance changes that would occur in **Panel A** with the infiltration of an H_2O-rich fluid at two different temperatures. **Panels 3-4** detail the modal abundance changes that would occur in **Panel B** with the infiltration of an H_2O-rich fluid at two different temperatures.

Figure 10: Volatiles isopleth diagram for an ophicarbonate composition (carbonated serpentinite) initially containing 5.5 wt. % CO_2 and 11.0 wt. % H_2O (composition modeled is based on sample G4 in Table 2 of Pelletier et al., 2008). Although such rocks experience significant dehydration over the 550-800˚C temperature range, relatively little CO_2 is lost and even the warmest of the *P-T* paths (Cascadia) results in only ~15% loss. Based on somewhat different bulk compositions, the calculations of Kerrick and Connolly (1998), with the *P-T* paths of Syracuse et al. (2010) superimposed, similarly indicate near-complete CO_2 retention in forearcs. However, relative to our calculations, the calculations by these authors indicate considerably higher (near complete) CO_2 losses along these more recently published paths for the depth interval of 80-120 km. The C input into subduction zones in this lithology is highly uncertain, with the estimates in **Table 1** indicating contributions of ~4-21 % of the total C inventory.

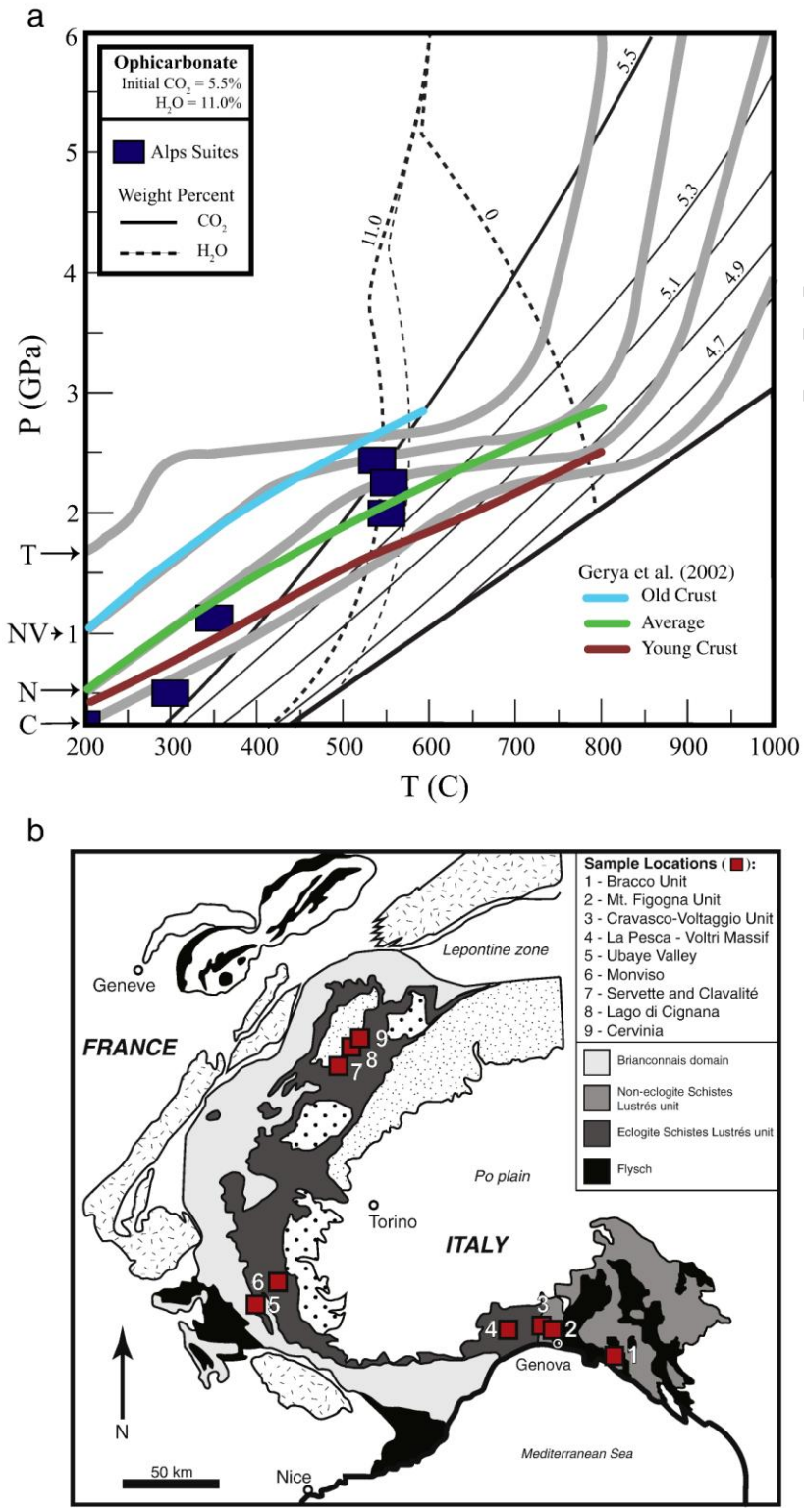

Figure 1

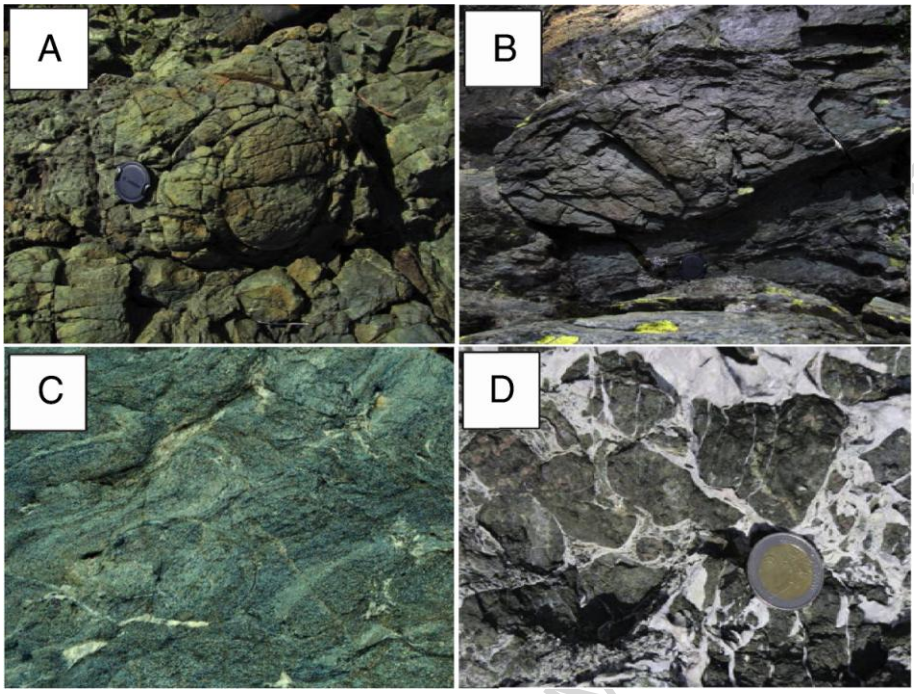

Figure 2

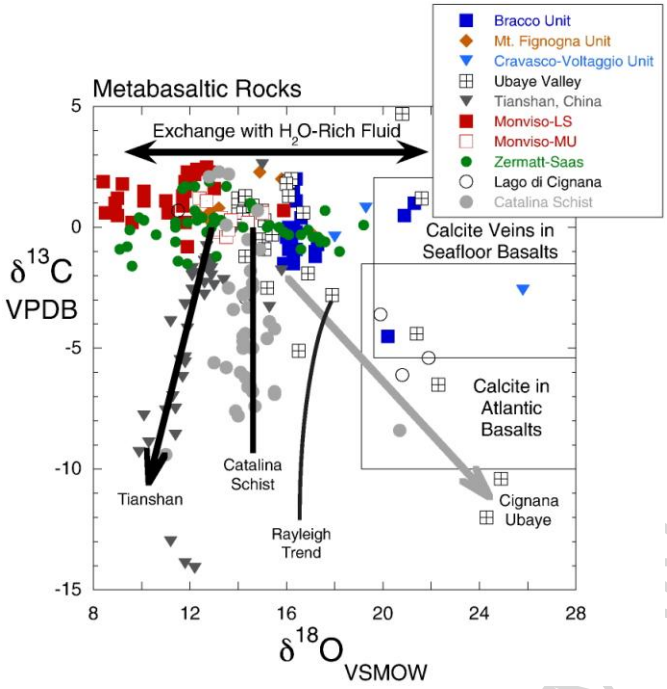

Figure 3

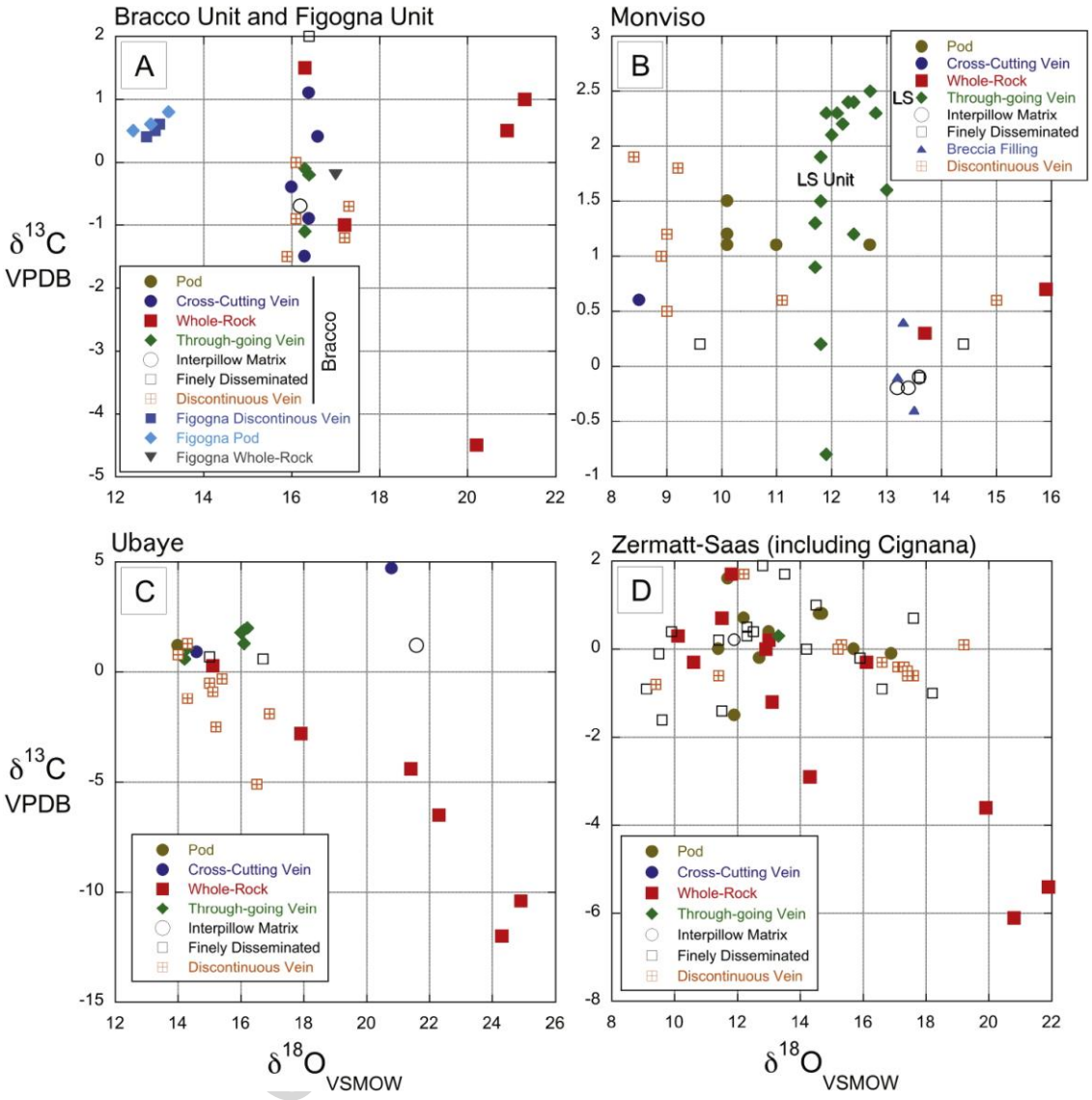

Figure 4

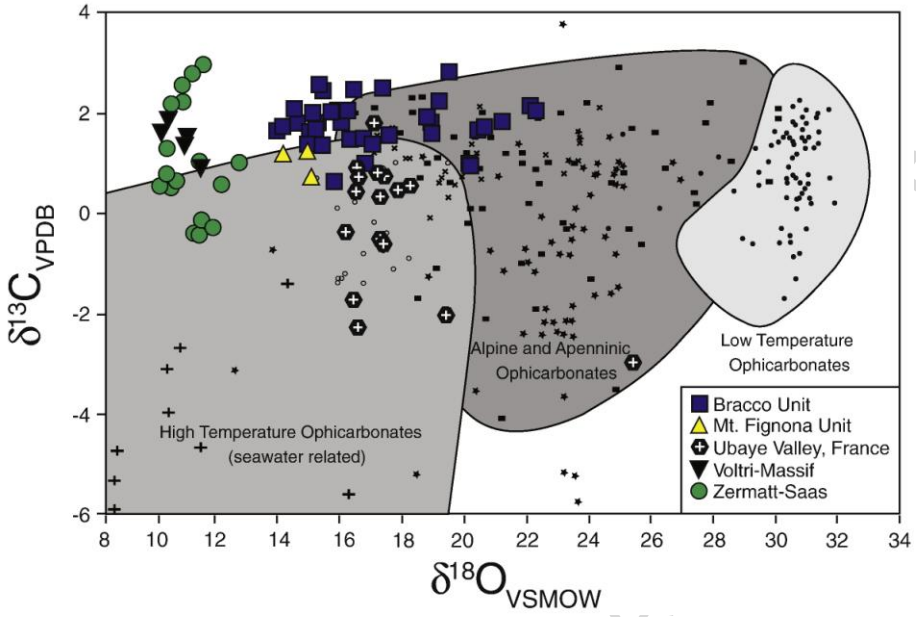

Figure 5

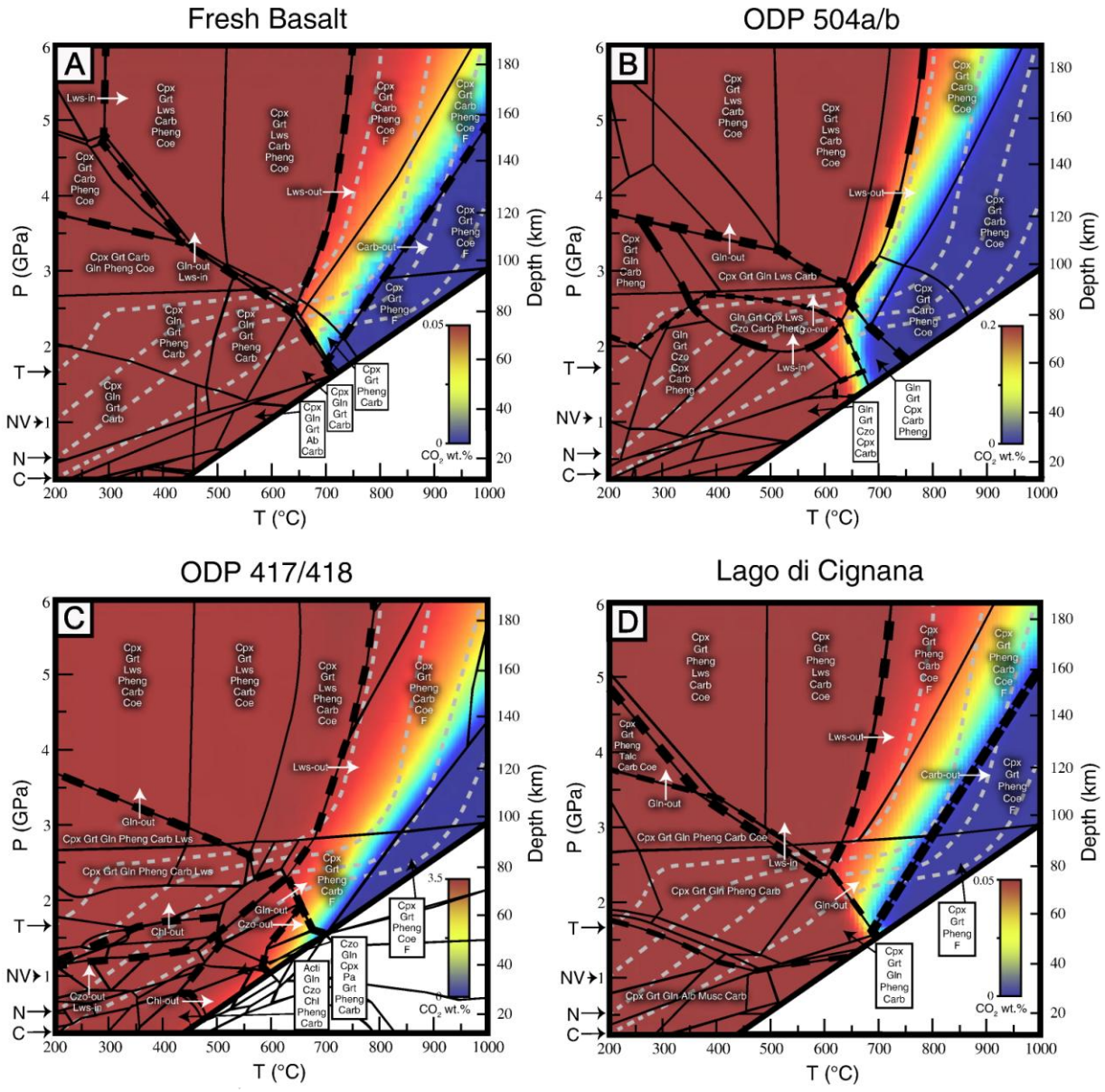

Figure 6

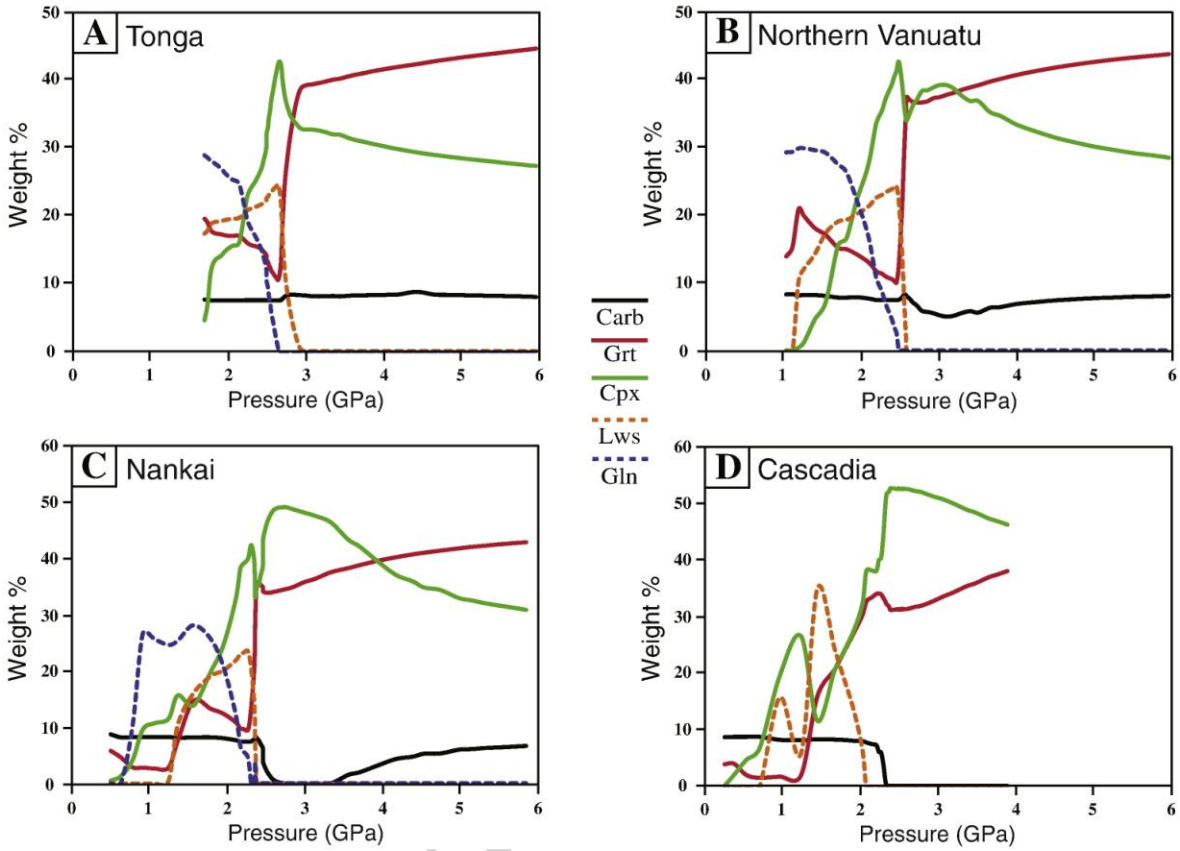

Figure 7

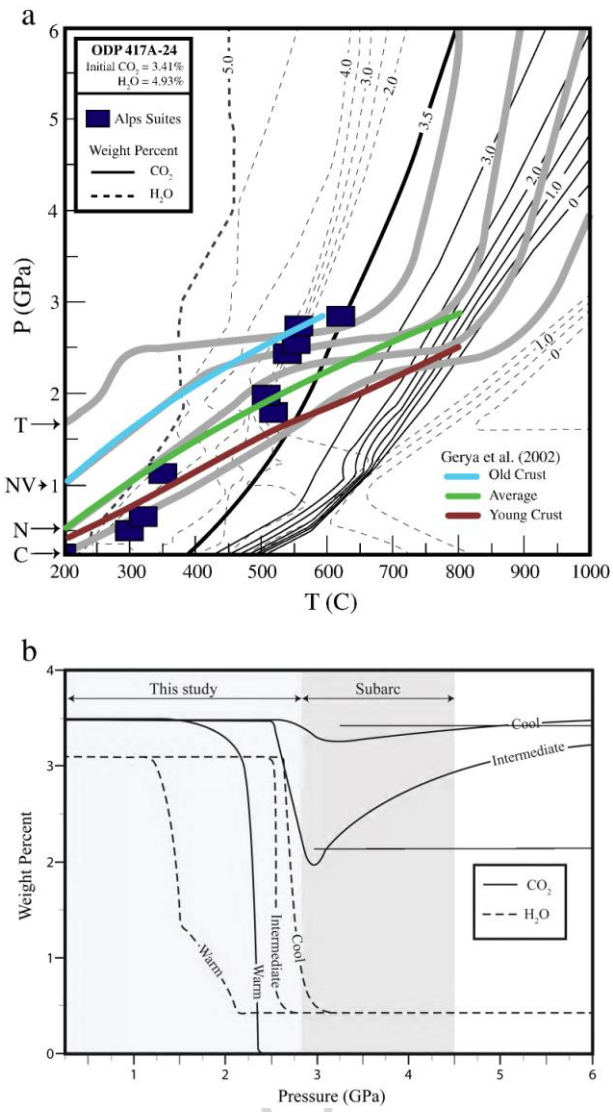

Figure 8

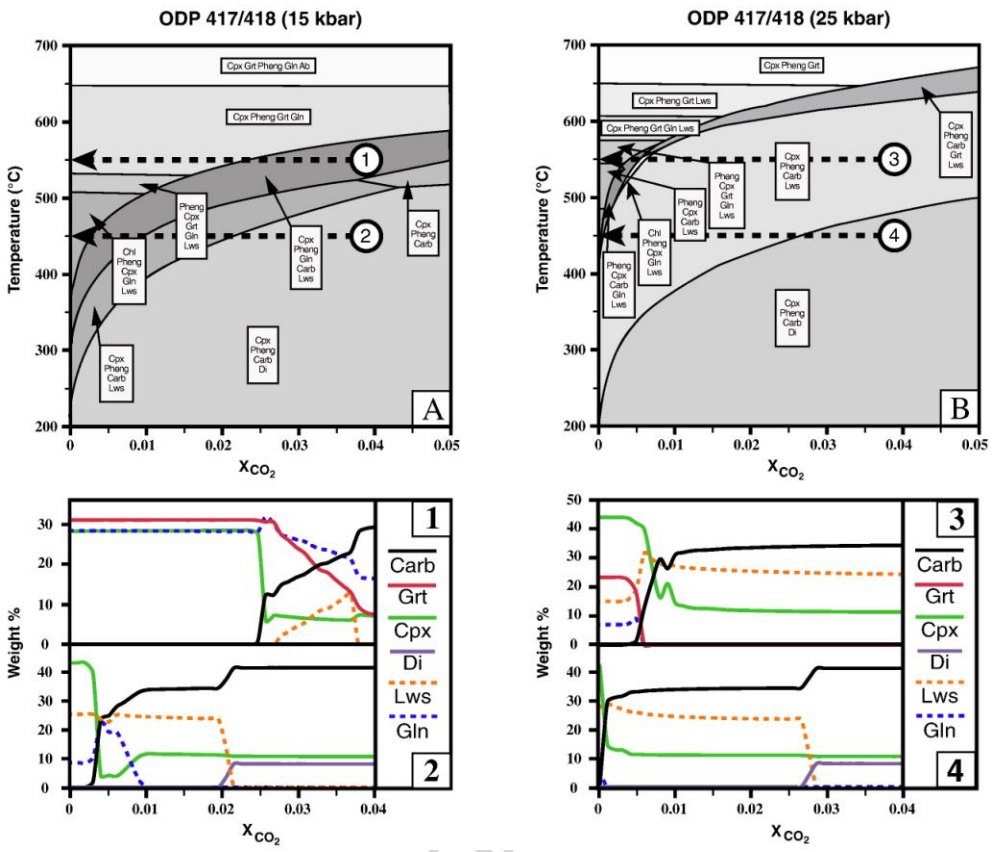

Figure 9

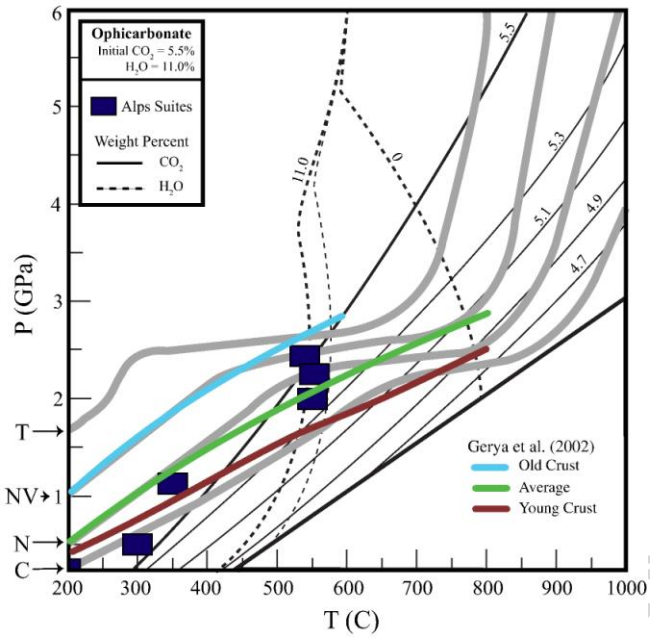

Figure 10

Table 1. Estimates of C subduction input and output fluxes from the recent literature.

Input (x 10^{12} mol C/yr)				
	Sediments	**Basalts**	**Ultramafics**	**Total**
Bebout (2007, 2014)*	0.9 - 4.8	3.1 - 4.0	*0.4 - 0.8***	*4.4 - 9.6*
Dasgupta (2013)	1.1 - 1.4	3.0 - 5.1	0.4 - 0.8	4.5 - 7.3
Hilton et al. (2002)	1.34	2.12	*0.4 - 0.8***	*3.86 - 4.26*
Jarrard (2003)	1.2	2.27		*3.87 - 4.27*

Output (x 10^{12} mol C/yr)	**Arc Gas**	**Return Efficency**
Varekamp et al. (1992)	1.5	16 - 80%
Marty & Tolstikhin (1998)	2.5	
Sano & Williams (1996)	3.1	

*The methods for calculating these fluxes are presented in Sadofsky and Bebout (2003).
**from Dasgupta (2013; this flux is added to the sediments and basalts estimates by the other authors)

Table 2. Textural settings of carbonate localities for which C and O isotope data are presented in this paper

Unit	Location	Interpillow Material	Outcrop-scale veins	Hand-sample scale veins
Bracco Unit	Zerli			
Bracco Unit	Foppo	XX	X	XX
	Porto Pidocchio	XXX	XX	XX
Mt. Figogna Unit	Figogna	XX		X
Mt. Figogna Unit	Pietra Lavezzara	XX		X
Cravasco-Voltaggio Unit	Lencisa	X		
Ubaye Valley, France	Pic du Pelvat	XXX		XX
Lago Superiore Unit	Monviso	X	X	XX
Monviso Unit	Monviso	XX		
Zermatt-Saas Ophiolite	Cervinia	XXX		
Zermatt-Saas Ophiolite	Servette	XX		X
Zermatt-Saas Ophiolite	Clavalité	XX		
Zermatt-Saas Ophiolite	Lago di Cignana			

X - Present XX - Readily Available XXX - Abundant

Table 3. Extents of Loss of CO_2 in 80-120 km Depth Range, Closed - System Models Only (Figs. 8A, 10; Kerrick and Connolly, 2001a)

	Cascadia	**Nankai**	**N. Vanuatu**	**Tonga**
417A-24 (basalt)	100%	100	43	7
Ophicarbonate	15	13	7	3

Sediment Composition
(from Plank and Langmuir, 1998)

GLOSS	100	100	100	29
Antilles	100	100	100	61
Marianas	17	10	7	2
Vanuatu	23	13	6	0

Research Highlights:

- Effects of subduction zone metamorphism on C cycling were examined.

- Calculated decarbonation history matches observed reaction history.

- Subducting metabasalts and ophicarbonates retain most of their C to 90 km depths.

- Metabasalts largely retain seafloor-inherited carbonate C isotope compositions.

- Extent of CO_2 retention depends upon degrees of infiltration by H_2O-rich fluids.